



A Medical Device for Tracking Peripheral Edema in Patients with Chronic Heart Failure

Team Members:

Christian Duffy de Abreu

Fabian Louis

Léo Kensicher

Nikhil Krishnan

Bernardo Penteadó

Alejandro Villasmil

Faculty Advisor:

Dr. Mark Yim

Final Project Report

MEAM 445/446, MEAM Senior Design

September 2017 - April 2018

April 30th, 2018

Team 02: Peri



Abstract

Peripheral Edema (PE), the swelling of the legs due to fluid retention, is clinically used to signal a worsening heart condition in Chronic Heart Failure (CHF) patients. The principle method of detection is pitting where a nurse indents the swollen limb using their thumb or index finger and observes the depth and rebound time of the resulting indentation.

This method is highly subjective as reported levels of swelling vary from nurse to nurse, and as nurses are not readily available at home, outpatients have to self-detect this increase in fluid retention by tracking their weights daily, a requirement that has been proven to have low patient compliance.

Peri, a sock-based technology that remotely monitors PE, eradicates these problems as the sock integrates seamlessly into the patients' life, thus maximising compliance, while also eliminating the subjectivity of pitting by employing sensors that track changes in leg circumference to detect fluid retention.

To realise the solution, the team built a radially expandable edematous leg model that facilitated sock compression tests with varied leg circumference, as well as tests for precision, accuracy, and repeatability of sensor readings. Tests were also run on industry standard edema training kits to determine mechanical (i.e., viscoelastic) properties of edematous tissue using a custom MTS machine that the team built to validate the accuracy of the leg model.

Further steps would include miniaturising the sock's electronics module and, after receiving IRB clearance, having CHF patients wear the sock to further validate the device's functionality and comfortability.

Table of Contents

1.	Executive Summary	5
2.	Statement of Roles and External Contribution	6
2.1.	Team Members	6
2.2.	Advisors	8
2.3.	Professional Contributions	10
3.	Background	11
4.	Objective	18
4.1.	Wearable Sensing Mechanism	18
4.2.	Leg Model	19
4.3.	Design Impact of Standards	21
5.	Design and Realization	24
5.1.	Ideation of Possible Final System Form	24
5.1.1.	Ankle Strap with Stretch Sensor and Integrated Feedback Module	26
5.1.2.	Sock with Stretch Sensors and Integrated Feedback Module	26
5.1.3.	Sock Embedded with Nanoparticles for Passive Color Feedback	28
5.1.4.	Insole with Load Sensor and Integrated Feedback Module	29
5.1.5.	Portable Electronic Pitting Device with Integrated Feedback Module ...	30
5.2.	Down Selection	32
5.3.	Overview of Project Components	34
5.4.	Custom MTS Machine	35
5.4.1.	Overview.....	35
5.4.2.	Manufacturing of Final System Form	36
5.4.3.	Final Design	38
5.5.	Leg Model	39
5.5.1.	Ideation	39
5.5.2.	Design Iteration	42
5.5.3.	Final System Form	44
5.5.4.	Manufacturing of Final System Form	46
5.5.5.	Final Design	51
5.6.	Sock	52
5.6.1.	Ideation	52
5.6.2.	Down Selection	53
5.6.3.	Final System Form	54
5.6.4.	Manufacturing & Testing of Final System Form	55
5.6.5.	Final Design	71
6.	Validation and Testing	71

- 6.1. Pressure Tests 71
- 6.2. Foam Model Validation Tests72
- 6.3. Sock Measurement Precision Tests 75
- 6.4. Power Consumption Tests 75
- 7. Discussion 77**
 - 7.1. Target versus Accomplished Performance77
 - 7.1.1. Sock 77
 - 7.1.2. Custom MTS Machine 78
 - 7.1.3. Leg Model 79
 - 7.2. Recommendations 79
- 8. Budget, Donations, and Resources 82**
- 9. Intellectual Property 84**
- 10. References 85**
- 11. Appendix 90**

1. Executive Summary

5.7 million Americans suffer from Cardiac Heart Failure and 660,000 new cases arise every year[1]. Over 80% of the direct costs related to heart failure are due to hospitalization and patients are expected to cover an average lifetime cost of around \$73,762[2]. Peripheral edema is a significant indicator of CHF, the early onset detection and monitoring of which could reduce hospitalization rates and prevent exacerbation of the condition. Today, methods of peripheral edema monitoring and diagnosis of patients with chronic heart failure are imprecise, resource-intensive, and not patient-specific[3]. The severity of an edema is dictated by the deviation of the patient's leg diameter, heart rate, and temperature from their baseline values, which require precise and on-the-spot tracking for effective diagnosis[4]. CHF patients require non-invasive monitoring solutions and maximized comfort above all.

With these considerations in mind, the team developed a medical device that detects presence of peripheral edema that allows for remote patient monitoring via wireless connectivity. The consistency measurement is more important than accuracy because, as stated above, diameter, heart rate, and temperature values are all measured from baseline values. Therefore, the device needs to consistently measure the variations from these base lines values to determine the changing health of the subject. The device consists of a patient-specific sensing sock that detects minimal changes in leg circumference along with alterations in leg volume. These are two main critical metrics involved in detecting this condition before any further heart failure complications ensue. In order to accomplish this, resistance band sensors are placed around the perimeter of the leg and used to sense any strain induced due to leg expansion. This signal is then filtered and collected by a microcontroller, where it can be processed and wirelessly transmitted. Another major component of the project involved designing and constructing an edematous mechanical leg model to test the device's accuracy and the reliability of its measurements. This allowed for ease of testing without human subjects. Pressure constraints imposed by the sock on the leg were also tested on this model. The team also developed a pitting device in order to gather viscoelastic properties of normal and edematous tissue, which are essential for the effective modeling of the physical leg model.

At the conclusion of the project, the team was able to design and construct a fully operational sock that can detect peripheral edema without disrupting the baseline diameter of the leg and the dynamics of the edema fluid. Furthermore, the team built and used a fully-functional leg model that closely mimics the viscoelastic properties of edematous tissue in order to perform testing procedures and validate the medical device.

The team accomplished two main goals in order to achieve the design of this sock. First, the strain sensors' ability to accurately and precisely detect changes in leg perimeter from baseline were tested.

The sensor readouts were then confirmed to be accurate in the sense that they return the same distraction produced on the mechanical leg. In addition, the values returned were verified to be repeatable and precise. Finally, the team will verified that the sock obeys the pressure constraints by recording the force and pressure applied by the device on the leg. This pressure was not less than the minimum pressure at which the device can sustain itself vertically. Furthermore, it did not exceed the maximum pressure at which the dynamics of the edema fluid are be significantly affected.

2. Statement of roles and external contributions

2.1. Team Members

Alejandro Villasmil

- MTS Machine development : Calibrated Load Cell
- Resistance Stretch Sensor Development/Validation: Conducted Measurement Precision Tests and Calibration Tests
- Sock CAD Ideation: Developed initial sock and module design CAD to aid in further development and presentations
- Edematous Tissue Foam Model Validation: Ran experiments with MTS Machine and high-density memory foam in order to validate the foam model with the corresponding edema grade (edema kits).

Bernardo Penteado

- Sock Manufacturing: responsible for sewing all components together
- Leg Prototype: responsible for CADing Telescoping Rods System and Radially-Expanding Arms System; responsible for 3D printing and laser cutting components and assembling the Telescoping Rods System and Radially-Expanding Arms prototypes
- Custom MTS Machine: responsible for designing and CADing prototype; responsible for conducting preliminary tests

Christian De Abreu

- Custom MTS Machine: designed and built circuitry for data collection; calibrated force and load sensors; authored Arduino script that controls the linear actuator speed and employs failsafes; worked on casing the MTS machine
- Leg Prototype: Fabricated the designed leg prototype; designed and built circuitry for leg prototype for pressure data collection
- Conducted sock pressure tests; gathered, analysed, and plotted data using MATLAB script developed

Fabian Louis

- Custom MTS Machine: conceived and designed the MTS machine; sourced electronic component for the MTS machine (i.e., load and displacement sensors, linear actuator); designed casing for MTS machine; worked on casing the MTS machine

- Leg Prototype: worked on designing the initial and final prototypes on Solidworks; developed the memory foam soaked in vegetable oil edema models models; performed pitting tests to validate the foam models
- Analysed and plotted data from pitting tests, moisture wicking tests, and heat dissipation tests

Leo Kensicher

- MTS Machine development: Defined required specs and selected system equipment, and helped develop and assemble the final system design
- Edematous Tissue Model: Worked on developing a Standard Linear Solid Model for viscoelastic tissue approximation (not used in final model). Conducted testing on Foam Models to approximate edema response to pressure.
- Comfort tests: Developed testing setup to evaluate sock comfort. Testing included moisture wicking tests on a variety of sock model bought off the market, as well as heat retentions tests.
- Patient outreach: Worked with Dr. Cacchione at Mercy LIFE Center to gather patient data and influence design choices for Sock Models and Custom MTS devices.

Nikhil Krishnan

- Custom MTS Machine: Soldered circuit and helped collect data
- Leg Prototype - Created Matlab script to detect and map the pressure distribution
- App - made wireless connectivity possible
- Designed original circuit design for sock
- Designed and ordered PCB using Eagle
- Sent all purchase orders

2.2. Advisors

Graham Wabiszewski

Dr. Graham Wabiszewski, professor of MEAM 445/446, was the main advisor to Peri, and gave structure to the efforts throughout the year. He provided guidance for presentations, timelines, and general work, and was very valuable given his experience teaching the class. In particular, his feedback on presentations, written assignments and more, drove the team to continually improve its work output to meet the expectations of the class throughout the course of the two semesters.

Dr. Mark Yim

Dr. Mark Yim was a technical advisor to Peri, and provided general guidance for the group throughout the year. This mainly consisted of advice regarding the electronics and intellectual property. More specifically, Mark showed the team several load cells for the pitting device, and helped the team select their final stretch sensor. He explained the pros and cons of WiFi vs BLE communication systems, helping the team decide on the latter. He also explained the process of acquiring a patent.

Dr. Pam Cacchione

Dr. Pam Cacchione, the Ralston House Endowed Term Chair in Gerontological Nursing, was also a technical advisor to Peri, helping the team with the medical aspects of the project. Dr. Cacchione presented the original idea of an edema tracking device to the team, and explained why edema is an effective metric for measuring chronic heart failure severity. Throughout the year, Pam has been very active for the team, taking full responsibility for organizing the expedited IRB, ordering the edema kits, and providing patients to interview regarding the device.

Wes Thomas

Wes Thomas was team Peri's assigned teaching assistant and advisor. He met with the team weekly, providing support and keeping the team on track. Given Wes' experience with senior design, he helped the team follow a specific timeline and helped find solutions for unexpected issues, such as the original leg prototype design not working, and certain ordered parts not arriving in time.

Dan Harris

Dan Harris, another teaching assistant for MEAM 446, provided the team with help regarding the PCB. More specifically, he looked over the design before ordering, and helped solder the tiny chips onto the board.

Genevieve Dion

Dr. Genevieve Dion, Director of the Center for Functional Fabrics at Drexel University, provided the team with advice regarding the design of the fabric of the sock. She explained how weaving patterns determine the elastic properties of fabric and offered her lab as a resource for the team to manufacture the sock. Unfortunately, in order for this to happen, the team and Dr. Dion needed to sign Non-Disclosure Agreements, which took too long to process, and the lab could not be used.

Sangeeta Vohra

Dr. Sangeeta Vohra, director of the Jerome Fisher Program in Management & Technology, advised the team mainly regarding the business side of the project, as Bernardo Penteadó is in the M&T program. She also put the team in contact with Dr. Ari Brooks (mentioned below) and gave her insights on intellectual property.

Ari Brooks

Dr. Ari Brooks, Professor of Clinical Surgery at the University of Pennsylvania, provided the team with advice from a doctor's perspective. He was present at all meetings with Dr. Vohra, and put the team in contact with several clinicians.

2.3. Professional Contributions**Sunstone Circuits**

Sunstone Circuits provided a free "manufacturability" test on the designed PCB, and manufactured the PCB within 24 hours.

Nursing SimLab

Nursing Sim-Lab provided the team with an artificial leg on design day, used to display the sock.

PennHealthX

PennHealthX provided the team with feedback from several successful entrepreneurs throughout the year and gave the team \$1000 dollars in funding to spend on the project.

Mercy-Life Hospital

The Mercy-Life Hospital provided the team with patients to interview regarding the device.

3. Background

The leading cause of death in the world is Cardiovascular Disease (CVD), a condition which includes diseased vessels, structural problems, and blood clots, and as such, represents an encombrant weight for healthcare systems around the world to carry[5]. And the US is not spared, as reports estimate that one American dies of CVD every 40 seconds[6]. Indeed, the American Heart Association (AHA) has made worrying projections regarding the expected presence of CVD - they foresee that close to 45% of Americans will suffer from a form of CVD by 2030, and that the medical costs surrounding CVD will skyrocket from under \$400 billion to \$918 billion[1]. On the bright side, however dangerous and widespread CVD may be, its severity can be reduced and often prevented when measures such as monitoring common risk factors in patients are taken. To the end of instituting positive change in this matter, the AHA has created the 2020 Impact Goal of the American Heart Association, in which it hopes to “improve the cardiovascular health of all americans by 20%” and “reduce the number of deaths from cardiovascular diseases and stroke by 20%”, by 2020[7]. An important concept upon which this goal relies, is that while medication may be central to controlling CVD, the patient's' diet and lifestyle changes will be vital to achieve success, hence the vitality of enabling clinicians to monitor patients both in hospitals and at home.

One of the most common forms of CVD is Chronic Heart Failure (CHF), which occurs once the heart is no longer able to meet the body's blood pumping demands for output. This usually begins with the Left Ventricle (LV), on the arterial side of circulation. As the LV loses function, blood flow slows down, especially in the body's extremities. LV failure begets Right Ventricle (RV) failure, as it increases the resistance to flow through the lungs, which leads to a degree of RV failure once it can no longer cope with the built-up pressures. This increase in pressure backs up the venous system, and as a result, when intravascular pressure exceeds interstitial hydrostatic pressure, fluid leaks out of the blood vessels and into the surrounding tissue - this phenomenon is known as edema. This occurs when the atrial volume receptors sense a decrease in effective atrial volume caused by the decrease in the heart's output. The atrial volume receptors, subsequently trigger nerve-mediated vasoconstriction in order to return to the right balance of heart output and vascular resistance. This effectively results in an increase in water retention[8]. As the pressure builds up, the work of gravity often results in edema occurring more heavily in the patient's lower extremities - this is known as Peripheral Edema (PE). There are several clinical indicators of CHF, including increased heart rate, increased respiration rate, and PE. There are over 20 million CHF patients in the world, including 5.7 million Americans[1]. Even more worrying are the 660,000 new cases of CHF diagnosed on a yearly basis, and the mortality rate of CHF patients, which has reached 287,000 per year. On average, half of CHF patients will die within 5 years of their CHF diagnosis.

CHF not only takes a toll on the population at large, but also on healthcare providers. Indeed, 11 million healthcare visits are related to heart failure each year alone, and heart failure hospitalization

rates exceed those related to cancer[1]. Furthermore, the cost of heart failure continues to rise, placing a heavy financial burden on the US economy and the health care system[9]. In 2012, the cost of heart failure to the US economy amounted to over \$31 billion, of which \$21 billion were direct costs. An impressive figure concerning direct costs, is that over 80% of the direct costs related to heart failure are due to hospitalization. Further studies have shown that in developed countries, 1% to 2% of healthcare spending are attributed to heart failure costs[2]. These costs are obviously also felt by the patients, who are expected to pay an average of \$110,000 in direct costs of their heart failure during their lifetime, a majority of which come in the form of hospitalization costs, which account for \$73,762 per person[2]. Furthermore, under the constraints of the Affordable Care Act, care providers now have to adapt to an environment heavily penalizing institutions with high rehospitalization rates[10]. Indeed, preventable rehospitalization rates have become an area of great concern as the healthcare industry desperately looks for new ways to cut costs. At least \$5 billion could be saved from avoiding hospitalizations and readmissions for chronically ill or frail elderly nursing home patients[11]. And this problem is very much present amongst heart failure patients, where some studies have shown rehospitalization rates for elderly patients that were close to 50% within 90 days of discharge[12]. Based on the admittedly subjective criteria of this study, 38% of those readmissions were judged preventable.

However, research has shown that CHF can be controlled with the implementation of self-care, and with potential clinical intervention. Because Peripheral Edema is a direct symptom of CHF, it represents a useful diagnostic marker for the severity of the disease, and as such, the condition of the patient may be monitored over time by tracking the state of their PE to assess the need for further clinical intervention. While PE may also be the manifestation of other less serious medical conditions, it should be noted that it is the main reason for rehospitalization for CHF[3].

The current methods of PE diagnosis rely mainly on a physical exam. The nurse or caretaker will compress the skin over the medial side of the tibia. If this leaves an indentation that recovers after a certain elapsed time, that is the diagnosis of edema. This is because usually there is no fluid between the skin and the surface of the tibia in a normal leg. Edema is graded from 1+ to 4+ by a variety of scales such as the one shown in Figure 3.1. In addition to there being variability amongst scales and characteristics of each grade of PE used by clinicians - the depth of the skin depression and the rebound time often vary from scale to scale - a significant problem in the current practice is the level of subjectivity upon which the diagnosis of edema relies, especially given that diagnoses may differ amongst clinicians. Clinical Nurse and Improvement Advisor of the Children's Hospital of Pennsylvania, Stephanie Ottemiller confirmed that at times nurses "instinctively known when it is a 2+". Dr. Jeffrey Berns, M.D. and Associate Chief of Penn's Renal and Hypertension department, reiterated the problem by saying that patients can be checked for edema by up to 9 different clinicians within the span of a day.

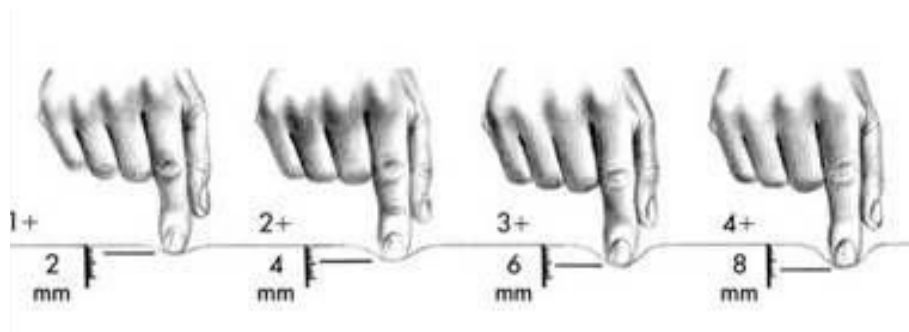


Figure 3.1: The Pitting Method for Diagnosing Peripheral Edema[5]

While there are some devices currently available to measure edema, they are expensive, inaccurate or impractical[4]. Furthermore, if a patient does not have access to the care of a nurse, which few CHF do outside of a hospital, doctors often rely on their patients to track their weight variation as a means for tracking PE - a surge in weight could signal a focused increase in water retention, signaling recurrent heart failure in its turn. However, this technique is intrinsically inaccurate as a variation in weight could be due to something as benign as a variation in the patient's level of activity, or simply a meal. Furthermore, patient compliance is also problematic, as many doctors find it challenging to extract accurate and consistent data from their patients[1]. Finally, a major issue with testing for PE by pitting is that, when dealing with patients who are overweight, it can be very challenging for the clinician to tell if the skin depression they are observing is due to the presence of PE or simply to the patient's larger size. This highlights the need for a baseline measurement from which to track variations in leg perimeter[13].

In light of the deficiencies of the current methods available to healthcare personnel, and following an interview that this senior design team conducted with Dr. Pamela Cacchione, Ralston House Endowed Term Chair in Gerontological Nursing & Associate Professor of Geropsychiatric Nursing, during which she shed her own experience on the matter and enumerated several general possible engineering solutions, the team set out to design a wearable device to accurately and remotely track peripheral edema. The need of the medical community expressed by Dr. Cacchione was that of a device that could eliminate the inaccuracy and subjectivity of the current practice of pitting, but further even, a device that would allow for accurate measurements remotely, and in a way that would be non-invasive and tailored to the patient. The benefits for the healthcare provider are the simplification of the resource intensive care-giving system, and a streamlined monitoring process. Furthermore, this would eliminate the disparate forms of diagnosis from when the patient is in the hospital or at home. Finally, the patients at home would not be bothered by an invasive device or a consuming practice that could increase their levels of stress and decrease their compliance, both of which would beget negative developments in their health.

It is worthwhile noting from the very start, that there is little, if any, direct correlation between clinical intervention and severity of edema, and that thus, an edema assessment by itself is irrelevant without information regarding the greater context of the patient's condition, meaning that two patients with the same measurement of edema may not require the same treatment[4]. Therefore, the purpose of the device that team set out to build would not be to replace a clinician to diagnose, but simply to provide them with more information to serve their diagnosis.

Furthermore, as the team learned during its exchange with Dr. Thomas A. Gillespie, MD FACC, the ability of a device to monitor remotely gives rise to the possibility of integrating predictive analytics to the system provided. While the immediate goal of the team was not to integrate predictive analytics into its system, it was clear that in the current climate of the medical device world, it was essential to design the team's solution such that it may serve as a foundation for predictive analytics in the future. Indeed, the benefits of such technology in this case are flagrant. As explained by Dr. Gillespie, "show the [clinician] a subtle change from the patient's baseline and [they] will have a better chance clinically heading off an exacerbation of HF and an unnecessary hospitalization. So, a change in condition for the worse can be analyzed, give the clinician a warning by remote monitoring, and allow early intervention before things get out of hand."

Substantial research concerning the detection and measurement PE has been conducted, including one comprehensive review of classic measuring methods by Brodovicz et al. that compared the reliability and level of correlation amongst clinicians assessing the PE[14]. The eight methods reviewed in this comprehensive study were a classic pitting test, a patient questionnaire, measuring ankle circumference, the figure-of-eight method for measuring ankle circumference, a plain edema tester comprising a plastic card with holes of varying sizes pressed onto the skin, a modified edema tester using bumps rather than holes, indirect leg volume measurement calculated from measuring ankle and leg circumference, and measuring foot and ankle volume by water displacement. The conclusion of the study was that water displacement and patient questionnaires were the most reliable method and had the lowest variability in diagnosis among clinicians. However, the methods also displayed significant drawbacks due to the time and preparation needed for implementation. While ankle circumference and patient questionnaires each took 1 minute to complete, other tools took over 5 minutes to complete. The methods used for this survey are described in more depth in Appendix A.

Based on the team's discussion with clinicians over the course of the project, the methods used in the study are not commonly used in the field as their slightly greater precision and reliability over the common pitting method are not great enough to warrant the setup or measuring time. It seems to be generally accepted that the potential increase in reliability is simply not worth the time or effort. Another very important point to note is that the tools used in these experiments were all derived from non-specialty components that anyone non-skilled in the art would be able to assemble at ease

for a total cost of under \$10., considering that the most expensive item in the study would be a plastic container with volume marks, enabling the clinician to detect a change in volume of the submerged lower leg. However, all of these tools also required the presence and expertise of a fully qualified clinician to conduct the experiments and make an experience-based assessment of the diagnosis.. Due to the significant variations in patient characteristics and in care providers, it is difficult to associate a single cost to the patient of having a clinician perform an edema assessment. However, an interesting study comparing the hospital, medical, pharmaceutical and nursing costs for older adults with heart failure showed that while accounting for the variability in the patients' needs and environments, the average cost of a single nursing intervention resulted in an increase in cost of \$289[40]. It follows that the greatest burden of cost for the heart failure patients arises from the need to have a nurse or other type of qualified clinician conduct an assessment of their peripheral edema. Thus any effort towards eliminating the need to have a clinician present as often while still monitoring the patient to the same degree could lead to significant reduction in cost for the patient.

PE may also be measured by probe depression measurements to present a reliable, accurate and quantifiable measure of a patient's edema, as is presented in US Patent #8425433B2 and in US Patent #6186962B1. Both of these patents essentially pit the patient while precisely tracking the depth of the depression with embedded strain sensors, leading to more accurate measurements.

Devices that measure edema via a spring-powered measuring tape system, comprising an optical encoder and a microprocessor[15]. The spring-powered tape method of measuring was found to be less accurate than an optoelectronic solution, which was ultimately chosen in this study despite its substantially higher cost and lower implementability. Furthermore, the experimentation was conducted by only one individual on two healthy patients, which eliminated variability between clinicians, and results on PE patients[16]. In fact, one study even found that by standardizing the tension and location of measurements, leg circumference measurements conducted with tape measurements could provide very reliable results[17].

As eluded to in the study by Brodovicz et al. PE measurement by water displacement can produce highly accurate results. A patent, US Patent #6077222A, describes a device allowing for such measurements, and even elaborates on the possibility of an automated version powered by the patient's own weight. However, this method also requires the existence of a baseline measurement, without which PE may not be detected, while the issue of the impracticality of this solution persists.

Another invention, US Patent #8744564B2 measures edema by comparing the ratio of extracellular to intracellular fluid of distinct body segments, a practice which relies on impedance measurements throughout different portion of the body. While this method offers high precision, it comes at the cost of practicality and cost. Bioelectrical impedance is also used in US Patent #6714813B2 to compare the limb's tissue to unswollen tissue.

Perhaps the most precise device for detecting PE currently on the market is an odometer, US Patent #5891059A, which details a device capable of using infrared sensing to scan a limb and calculate its volume. Here again, the high level of precision of this device comes at a price out of reach for many hospitals, nearing \$30,000. While such technology requires little preparation once the device is set up, it does require the patient to be mobile, which many patients are not.

One study identified the potential in using 3D imaging to remotely monitor heart failure patients by combining 3D imaging of the limb, body weight and limb circumference[18]. While the study offers a promising outlook, it still lacks the experimentation needed for proof of concept, and would rely on an extensive in home setup, which may limit this product's reach, as well as deter patients from complying.

Another invention elaborates on a handheld device, US Patent #8147428B2, that, when indenting the limb under an applied pressure, evaluates the stiffness of the underlying tissue. By creating a 3D model of the limb and comparing the stiffness measurements to the type of tissue (muscle, bone, etc.) where the stiffness test was conducted, the factors affecting indentation can be evaluated following a CT or MRI scan. The need for such equipment highlights the unsuitability of this method for any application beyond research[14].

Also, using dielectric electro-active polymers has been shown to lead to particularly valid measurements, and that in a relatively unobtrusive way to the patient[19]. Indeed, as this method applies relatively low pressure to the limb in question, it increases the overall reliability of the measurements.

Finally, throughout the course of the project, the team met with current Chronic Heart Failure Patients to gain a better understanding of their needs, notably at the Mercy LIFE Health System Center under the surveillance of Dr. Pamela Cacchione. It was important for the team to be able to devise a solution to the problem knowing the perspectives of both major stakeholders of the final product, that is the clinicians using it to perform a peripheral edema assessment, but also the perspective of the patients. The feedback received on many accounts showed a desire from the patients for their caregiver to be as well equipped as possible to give them an accurate assessment. However another component to the requests was that patients wanted something that was not invasive on their lives, and that did not require them to learn or perform experiments on themselves. One of the team's realizations during this process was that the majority of the Chronic Heart Failure patient population was among the elderly, which comes with its own set of challenges. Indeed, this requires a solution that would be extremely simple to use and that would not any type of movement or exertion beyond what would be considered part of a normal daily routine for these patients, many of whom explained that simply bending down can be a challenge.

This review of currently available solutions points to a void of any device or method capable of reliably, practically and cost-effectively remotely monitoring PE in CHF patients, and hence the need thereof. The small sample sizes, limited tests on real PE patients, lack of variability in device users, and impracticality of many of these solutions expresses a plea for innovation. The resulting invention would provide a standardized method for streamlining healthcare from clinician to CHF patient and help detect and prevent the aggravation of their state.

4. Objectives

Table 4.1, Table 4.2, and Table 4.3 below outline the project's basic and reach objectives for the Wearable Sensing Mechanism, Leg Model, and Custom MTS Machine respectively.

4.1. Wearable Sensing Mechanism

Table 4.1: Goals of Subsystem 1: Wearable Sensing Mechanism

Type	Description	Quantitative Goals
Reach	Measurement Precision	Precision of 6.3mm
Reach	Price	<\$100
Reach	Connectivity to Controller	Wireless
Reach	Washability	Washable with no user interference
Basic	Measurement Precision	Precision of 12.6mm
Basic	Maximum Pressure	8 mmHg
Basic	Price	\$150
Basic	Connectivity to Controller	Wired
Basic	Communication System	Bluetooth
Basic	Washability	Washable
Basic	Comfortability and Breathability	High user satisfaction

The team determined that the basic detectable variation in the leg radius must be 2 millimeters, given that this variation represents a change in edema level in conventional scales. Therefore, the system's sensors must be able to detect a variation of 12.6 millimeters in leg circumference ($2\pi r$). The reach

goal was to detect 1 millimeter variations in radius, representing a 6.3 millimeter variation in circumference.

Furthermore, if the device is to measure the diameter of the leg, then it must not affect that diameter. In other words, the device should not constrain the leg to the point of affecting the dynamics of the edema fluid, decreasing its diameter. According to research [58][59], the maximum allowable pressure on a leg before it experiences long term reduction in diameter is around 8 mmHg.

In terms of the device cost, the team came to the conclusion that since more and more medical devices are being designed with lay users in mind it would be wise to have a final price in an affordable range to the average Chronic Heart Failure Patient[60] . The device will also be sold directly to consumers, rather than to hospitals or insurance companies first. With this in mind, the team came a objective of \$150.

Another objective that was considered was the connectivity between the stretch sensor and electronics module. This was directly linked to the “washability” objective. The optimal results in this case would be to implement a wireless system or a system that would not interfere with the washability of the sock, as this might become a nuisance for the user. A system that does not have to rely on user intervention to make the sock washable would be the optimal objective in this case. This was declared a reach goal, while making the sock washable was considered basic.

Lastly, another main objective was implementing a communication system capable of relaying the sensor measurements to an end-user. The main purpose of this wearable sensing mechanism is to bridge the gap in chronic management of Peripheral Edema between patient and physician via remote monitoring. These measurements could also be relayed to close family members or friends via an external application. In order to accomplish this, the team determined a basic objective of implementing a Bluetooth LE system to communicate the sensor measurements with an end-user.

4.2. Leg Model

Table 4.2: Goals of Subsystem 2: Experimentation Apparatus - Leg Model

Type	Description	Quantitative Goals
Basic	Radial Expansion Range	3.5 cm to 7.3 cm
Basic	Minimum Pressure Measurable	~8 mmHg
Basic	Edematous Lamination on Leg Exterior	Laminate Leg Prototype Exterior with artificial 0 to 4+ Edema

The Leg Model is a physical experimentation apparatus that the team devised in order to validate the Wearable Sensing Mechanism described above. The team planned to wrap the leg model in artificial edematous tissue and measure the pressure values around the leg in order to validate the pressure exerted on it from the wearable sensing mechanism. The device required an adjustable circumference in order to resemble the different grades of edema present in Chronic Heart Failure patients.

For similar reasons to the Wearable Sensing Mechanism subsystem, the basic and reach characteristics for precision of leg perimeter adjustment in the leg model were set to 12.6 and 6.3 millimeters respectively. In addition, the team requires that the leg model be able to sense pressure differentials of 2 mmHg, which is 10% of the pressure applied by the average conventional compression sock[20]. However, it would be extremely beneficial to improve that precision to 1 mmHg for testing purposes.

Moreover, as already mentioned, the Leg Prototype should be able to simulate different grades of edema for different leg sizes. Therefore, it should be able to adopt different radii in a continuous range of values. According to a foot and ankle sizing survey[61] (see Appendix B for sizing chart), the baseline circumference of an adult leg (sizes M to XXL) around the region of the medial malleolus ranges from 22 to 30 cm, which would translate to a radius range from 3.5cm to 4.8cm. In order to account for the effects of peripheral edema, one should add one full inch in radius (2.5cm) to account for the maximum possible radius of the leg, which would happen at Level 4 edema. Therefore, the appropriate radius range for the Leg Prototype would be from 3.5cm to 7.3cm, which the team identified as basic requirements of the device.

Table 4.3: Goals of Subsystem 3: Experimentation Apparatus – MTS Device

Type	Description	Quantitative Goals
Basic	Range of Normal Operating Force	0 N to 10 N
Basic	Resolution of Force Measurements	~0.01 N
Basic	Displacement Range	0mm to 10mm
Basic	Resolution of Displacement Measurements	~2mm
Basic	Indentation Speed Control	Controllable Speed with the range of 0 mm/s to 3 mm/s

The team manufactured a MTS device that gathers force and displacement data of materials. This was used on different kits aimed to model the various grades of edema severity in the hopes of then using this data to validate the resemblance of the leg model to edematous tissue.

For the MTS device, the displacement range was chosen to be 10 millimeters, which represents a level 4+ edema. Similarly to the leg model testing apparatus, the measurement precision of this device must be at least 1 millimeter.

4.3 Design impact of standards

A barrier between any medical device and the general market is the U.S. Food and Drug Administration (FDA). The FDA currently categorizes medical devices into three classifications:

- Class 1 - General Controls (47%)
- Class 2 - General Controls and Special Controls (43%)
- Class 3 - General Controls and Premarket Approval. (10%)[22]

Class 1 devices are generally considered very low risk and thus have less regulation standards than devices in the other classes. An example of a Class 1 device is dental floss, where the patient has practically no risk of danger. Devices in Class 2 are considered higher risk than those in Class 1 and have more extensive regulations standards. Therefore, these devices require reasonable assurance of the safety and effectiveness of the product before going to market. An example of a Class 2 device is a thermometer, where an inaccurate body temperature measurement could result in an unneeded hospitalization, or worse, an oversight of a possible illness. Within the two classifications, Class 1 and Class 2 devices are further split into two categories: “exempt” and “not exempt”. The term “exempt” means that the product is exempt from 510(k), a pre-market submission that shows the FDA that the product is safe and effective, and/or exempt from Good Manufacturing Practices (GMPs), which requires that the product is manufactured consistently at quality standards. More specifically GMPs have the following main requirements:

- Adequate labor conditions
- Clearly controlled manufacturing processes
- Consistently recorded manufacturing records

Products exempt from the 510(k) are devices that existed in some form before the 510(k) was established on May 28, 1976, and have not significantly changed since then[23]. Class 2 devices can never be exempt from GMPs. Class 3 makes up only 10% of medical devices and includes the

products associated with the greatest risk. An example of a Class 3 device is a pacemaker, whose effectiveness can be the difference between life and death of a patient.

Due to its relation to CHF, this device immediately poses too much risk to be classified as Class 1. To help with the categorization of medical devices, the FDA has a Code of Federal Regulations (CFR), where it further breaks down devices into categories with specific classes. Under the listed category, “Cardiovascular Monitoring Devices”, every device is considered to be Class 2 [24]. This is likely where the edema tracking device would fall, but as none of the existing categories are related to edema, it is hard to know for certain. Instead, the device more closely resembles a Physical Diagnostic Device, more specifically, a force-measuring platform, which converts pressure readings into a digital/electronic signal. Overall, the device likely falls in the crossroads between a cardiovascular monitoring device and a Class 1 force-measuring platform and does not impose enough risk on the patient to be considered a Class 3 device[23].

As this device is Class 2 and no existing similar classified products existed before May 28, 1976, it would not be exempt. Unfortunately, this would require a 501(k) to be approved by the FDA, which costs on average \$24 million dollars. This money mostly is spent on studies that show the device is effective [25].

Testing the product on actual patients with edema would require obtaining Institutional Review Board (IRB) approval. The FDA requires IRB approval for research projects involving human subjects in order to protect the rights of the research subjects and ensure their safety. Due to the medical fragility of those with CHD and potential severity of the disease, IRB approval of any product tests and research on its effectiveness will be a critical component to both protect the patients and reinforce the validity of the findings. Gaining IRB approval can be a time-consuming and difficult process and presents a potentially formidable barrier to the project’s success. In order to mitigate this risk, Dr. Pamela Cacchione, PhD, Ralston House Endowed Term Chair in Gerontological Nursing & Associate Professor of Geropsychiatric Nursing, has guided the team through the approval process. Furthermore, the product presents no substantial risk to patients, particularly in its use as a screening device for edema risk as opposed to a diagnostic or treatment tool. These factors mitigate concerns surrounding obtaining IRB approval. A request for IRB approval was submitted on 3/12/2018, the outcome of which is still unknown at the time of this publication.

Since the team wanted to include in its design that it would likely be working with patients in the future and as part of the IRB approval process, it was also important to be cognizant of limitations imposed by the Health Insurance Portability and Accountability Act (HIPAA). The HIPAA Privacy Rule establishes certain personal identifiers as protected health information (PHI) that must remain entirely confidential. PHI includes the following categories of information: Patient names ; Addresses more specific than state of residence ; Dates, including birth, discharge, admittance, and

death dates ; Telephone and fax numbers ; Email addresses ; Social Security numbers ; Driver's License information ; Medical record numbers ; Account numbers ; Health plan beneficiary numbers ; Certification/license numbers ; Vehicle identifiers and serial numbers, including license plate numbers ; Device identifiers and serial numbers ; Names of relatives ; Internet Protocol (IP) address numbers ; Biometric identifiers ; Full face photographic images and any comparable images[26]

As with any work with patients in the healthcare field, all of the team's efforts were in compliance with the HIPAA Privacy Rule both for IRB approval and more generally throughout each stage of the project involving patients. As such, the team always avoided collecting or recording any of the above-listed PHI.

Furthermore, in given the number of suggestions leaning towards a wearable device before the team began the design process, the team also wanted to make sure that it was aware of current engineering standards that may apply to that specific type of device. The team's objective was to build a device that sustains or offers general improvement to functions associated with a general state of health while referring to diseases or conditions, or more specifically a device that may help to reduce the risk of certain chronic diseases or conditions, including the transmission medical data. The wearable device would thus qualify as a "General Wellness" device as defined by the FDA and thus fall under the lowest category of scrutiny[41]. Given the device's other characteristics mentioned above, it would require any additional levels of testing to be approved. Based on the above, there would be no specific extra regulation regarding textile standards for the product if the measuring device is embedded in an item of clothing as long as they abide by the rules set forth by the FDA in Sec. 177.2800 Textiles and Textile Fibers. If the wearable device route were chosen, this would allow the team to include materials from regular apparel on the market. Slight modifications could be included according to current standards, such as using copper-infused fabric for its antimicrobial properties, which would still comply with the standards listed above[42]. Given that the team will also likely be using electronics in the chosen solution, it would be required to abide by ISO 14971, which is an ISO standard for the application of risk management to medical devices that sets guidelines for design while being cognizant of the use-based risk associated with human interaction with the mechanical and electrical components if a system[43].

5. Design and Realization

5.1 - Ideation of Possible Final System Form

As previously introduced, Peripheral Edema (PE) is a strong indicator of a worsening heart condition in Chronic Heart Failure (CHF) patients, and thus the ability to precisely and accurately track the onset and progress of PE would allow for appropriate medical interventions to be employed, in a timely manner, that would effectively prevent both the recurrence of acute CHF, and also rehospitalizations.

Available literature has revealed various parameters that could be measured to assess the severity of PE. The various methods and their associated measured parameters can be classified into those that track changes of the external, or the internal properties of the edematous tissue, and also those that measure the mechanical response of edematous tissue subjected to external loads.

These types are presented as follows[44]:

1. Type 1: Methods that measure the external properties of the body and/or of the edematous tissue;
 - 1.1. Measuring the change in ankle circumference with time
 - 1.2. Measuring the change in leg volume with time
 - 1.3. Measuring the change in body weight with time
2. Type 2: Methods that measure the internal properties of the edematous tissue;
 - 2.1. Measuring the bioelectrical impedance of edematous tissue to determine the ratio of intercellular to intracellular water content
 - 2.2. Using Ultrasound or Magnetic resonance Imaging (MRI) to produce an accurate picture of the internal composition of the edematous tissue
3. Type 3: Methods that measure the mechanical response of edematous tissue subjected to physical loads
 - 3.1. Measuring the resistive force of edematous tissue when applying an external force
 - 3.2. Measuring the indentation depth of edematous tissue after applying force
 - 3.3. Measuring the rebound time of edematous tissue after indentation

For purposes of the Senior Design project, solutions that employ the methods described under Type 2 were ruled out because of time, financial, and legal constraints, as described herein.

Firstly, the realisation of such solutions would be expensive because of the costly nature of such technologies, and also prototyping a device which employs these technologies would require a lot more time than is allocated for the project.

Secondly, assessing the performance of said prototyped devices would require testing and calibration on live patients exclusively as artificial edematous tissue does not possess the same properties found in live tissue. As such, a legal permit, e.g. an IRB, would be required. Acquiring the permit would further increase the time cost as it is a bureaucratic process, and in the event that the permit is not approved, assessing the performance and calibration of the prototype would not be possible.

Another important factor to be considered, although long term, is patient compliance. For instance, for a prototype that uses the principle of bioelectrical impedance, the method of PE assessment would require the conduction of low strength high frequency currents through the edematous tissue via electrodes. Although the current conducted is of extremely low strength, in the order of 10^{-6} A, patient compliance is expected to be a problem[44]. Therefore, for the reasons detailed above, solutions that employ the methods described under Type 2 are impractical for the project.

The solutions that remain are therefore those that employ methods described under Types 1 and 3, i.e. the methods for tracking PE that monitor the external properties of edematous tissue, and those that measure the mechanical response of edematous tissue subjected to physical loads, respectively.

In addition, to make remote monitoring of PE practical for both the patient and the doctor, as well as to improve patient compliance, it was reasonable that the optimal solution should be a smart wearable device that would require minimal or no reliance on the patient for operation. This approach minimises the human error that would result from a manually operated device, and would also be accessible to outpatients who would otherwise require a skilled practitioner to operate a manually operated device.

Following the rationale above, the following potential system level solutions were devised:

1. Ankle strap with stretch sensor and integrated active feedback module
2. Sock with stretch sensor and integrated active feedback module
3. Sock embedded with nanoparticles for passive color feedback
4. Insole with load sensor and integrated active feedback module
5. Portable Electronic pitting device with integrated active feedback module

For the active feedback system level solutions identified above, the functionality would perform as illustrated below;

A sensor measures a change in a specified property and outputs an analog signal. The analog signal is converted into a digital signal and filtered for noise by a microprocessor. The filtered digital signal output is then sent to a Bluetooth module which wirelessly broadcasts it to a central server. The signal broadcasted to the central server would be further processed, analysed, and interpreted with software into a useful output value for the end-users, i.e. the patients and medical personnel.

5.1.1 - Ankle Strap with Stretch Sensor and Integrated Active Feedback Module

The ankle strap is illustrated in Figure 5.1 below. The proposed device will have the ability to track the progression of PE by actively measuring and reporting the change in the ankle circumference. For consistent measurements, the ideal position for measuring the ankle circumference for purposes of assessing PE is approximately 7 cm above the medial malleolus[45].

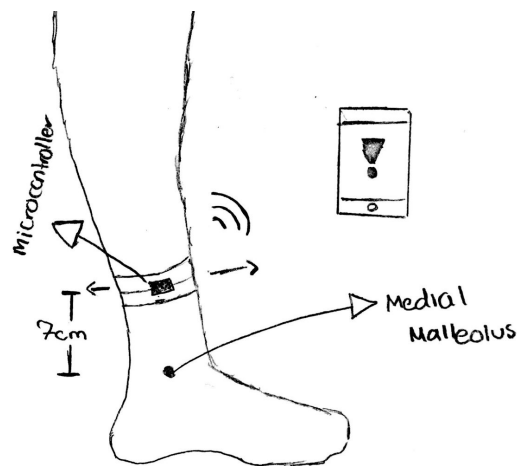


Figure 5.1: Ankle Strap with Stretch Sensor and Integrated Active Feedback Module

5.1.2 - Sock with Stretch Sensors and Integrated Active Feedback Module

Figure 5.2 below illustrates concept drawings of the proposed socks designs that are equipped with stretch sensors and integrated active feedback modules.

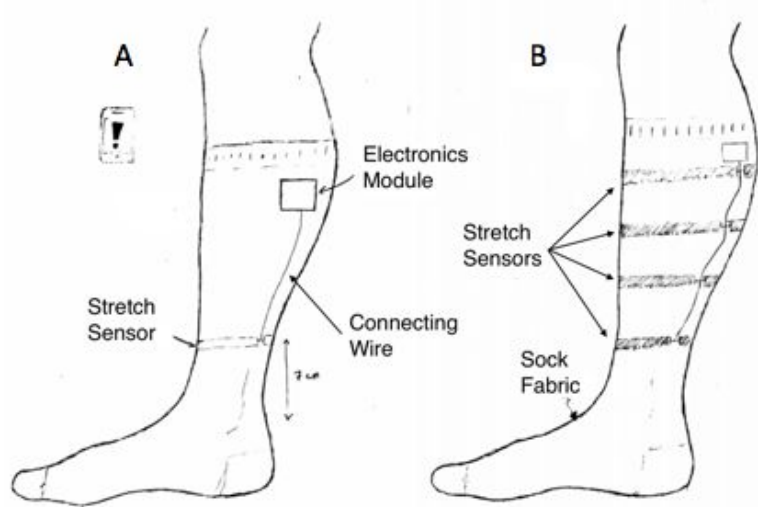


Figure 5.2: Sock with Stretch Sensors and Integrated Active Feedback Module

The functionality of the sock illustrated in Figure 5.2(a) is primarily similar to that of the aforementioned ankle strap. Alike the ankle strap, the sock's stretch sensor measures the changes in circumference of the edematous leg over time, and is positioned at approximately 7 cm above the medial malleolus for consistent circumference measurements.

Figure 5.2(b) illustrates a variation in the sock proposed in Figure 5.2(a). The sock shown in Figure 5.2(b) utilises n stretch sensors distributed along the leg of the sock and therefore measures changes in circumference over time at n distinct positions. This variation enables volumetric measurements of the edematous over time via the use of the Frustum Method. Kaulesar *et al.* detail this methodology of volumetric measurement employed in PE assessment in a study on the direct and indirect methods for the quantification of leg volume[46].

The formula presented in Equation 5.1 below illustrates how leg volume can be obtained from n leg circumference measurements.

$$V_{total} = V_1 + V_2 + \dots = \frac{h}{12\pi} \{(C_1^2 + C_1C_2 + C_2^2) + (C_2^2 + C_2C_3 + C_3^2) + \dots\}$$

Equation 5.1: Leg Volume via the Frustum Method

Referring to Equation 5.1 above; h equals the length measured from the lowest stretch sensor to the top most stretch sensor, C_1 corresponds to the circumference measurement recorded by the lowest stretch sensor, and C_2, C_3, \dots , correspond to the circumference measurements of the n stretch sensors above the lowest stretch sensor. V_1, V_2, \dots , represent the volumes of the frustum segments bounded by the stretch sensors. Much like the sock illustrated on **Figure 5.2(a)**, the lowest stretch sensor of the sock would be positioned at approximately 7 cm above the medial malleolus.

5.1.3 - Sock Embedded with Nanoparticles for Passive Color Feedback

Coloration in nature could be explained as a consequence of the interaction of light with complex nanostructures. These so called structural colors can exist without the presence of dyes because of the photonic band gap of ordered structures[47]. Such patterns can be observed on beetles' exoskeletons or feathers of birds where light is scattered and reflected at specific frequencies which are perceived as different colors by the observer.

Furthermore, photonic crystals that scatter said light are anisotropic in structure, i.e., the observed color also depends on the incident angle of light, a phenomenon known as iridescence. However, this would not be able to be incorporated into the sock. Instead, an engineered arrangement of nanostructures could result into non-iridescent color schema such that any angle of observation would result in the same color observed. Such scattering, known as Mie, yields light strongly scattered within a resonant frequency range due to electromagnetic properties outside the scope of this project but discussed by Wei *et al.* [47], and could be a potential solution.

Figure 5.3 below illustrates the concept. In this embodiment, the fabric changes color as discussed above as a result of stretching.

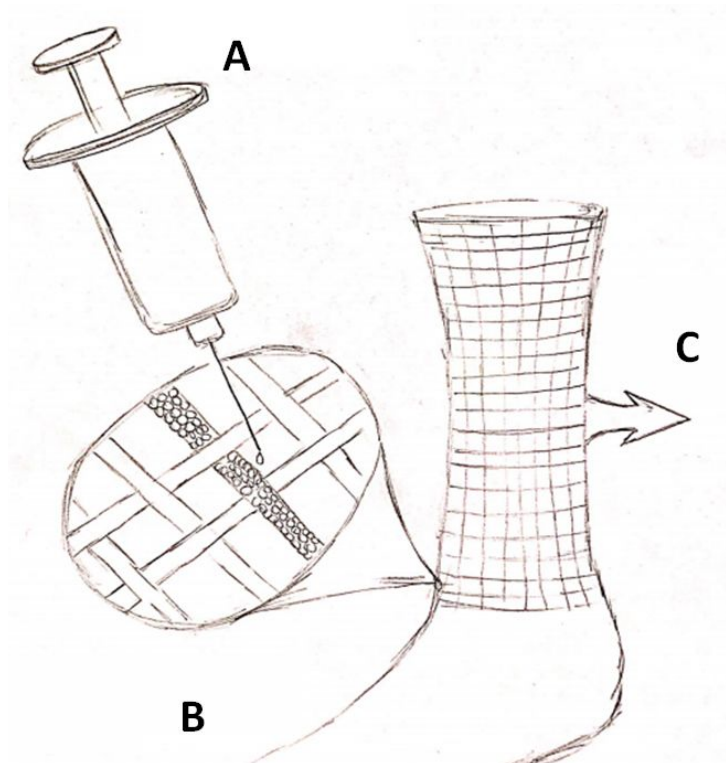


Figure 5.3: Sock Embedded with Nanoparticles for Passive Color Feedback

5.1.4 - Insole with Load Sensor and Integrated Active Feedback Module

The current clinical practice employed to track PE for the case of outpatients with CHF is the reporting of body weight measurements[48]. For CHF patients, body weight increases with the progression of PE as a result of an increase in the body’s fluid retention. With this practice, CHF outpatients are instructed by their clinicians to weigh themselves and report their weights twice on a daily basis; once after waking up, and once before going to bed.

To replicate and enhance the practice of daily weight measurements, an insole with built-in load sensors and an integrated active feedback module was proposed. The load sensors would be strategically positioned to ensure accurate and consistent measurements of weight over time. The positioning of the load sensors is dictated by the locations of anticipated maximum pressure points exerted by the foot onto the insole when the patient is either walking or standing. These maximum pressure points correspond to those observed on plantar pressure maps of the foot generated during static plantar pressure mapping tests (i.e., when standing) and dynamic plantar pressure mapping tests (i.e., when walking) as shown in Figure 5.4 [49] below.

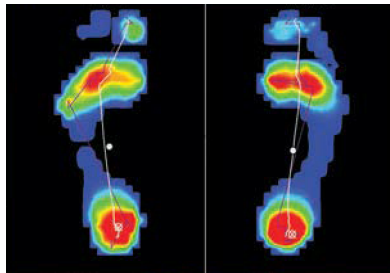


Figure 5.4(a): 2D Static Plantar Pressure Map

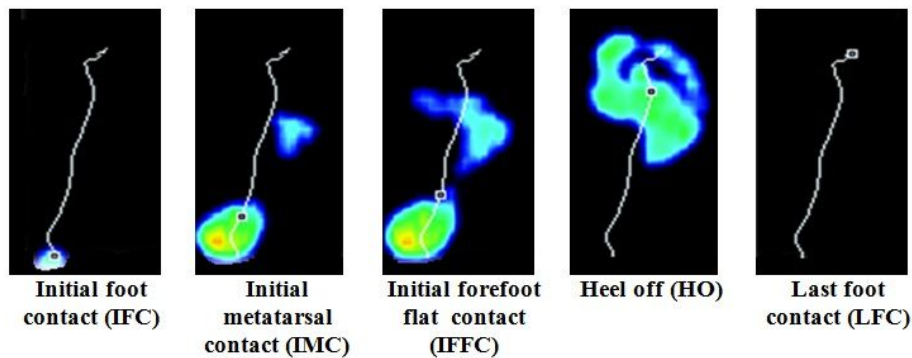


Figure 5.4(b): 2D Dynamic Plantar Pressure Map

Referring to Figure 5.4 above, the load cells would thus be positioned at locations on the insole where the heel and the ball of the foot rest upon as these locations would experience the maximum exerted pressures (red corresponds to higher pressure in the maps). The maps presented in Figure

5.4 above were obtained from a healthy adult who exhibits a proper standing and walking form. However, the mechanics of walking varies greatly within a population, and thus the accuracy and consistency of weight measurements would benefit from averaging facilitated by the use of multiple load sensors.

In the first embodiment of the insole design, two load sensors are positioned at the locations specified above; Figure 5.5 below further illustrates this.

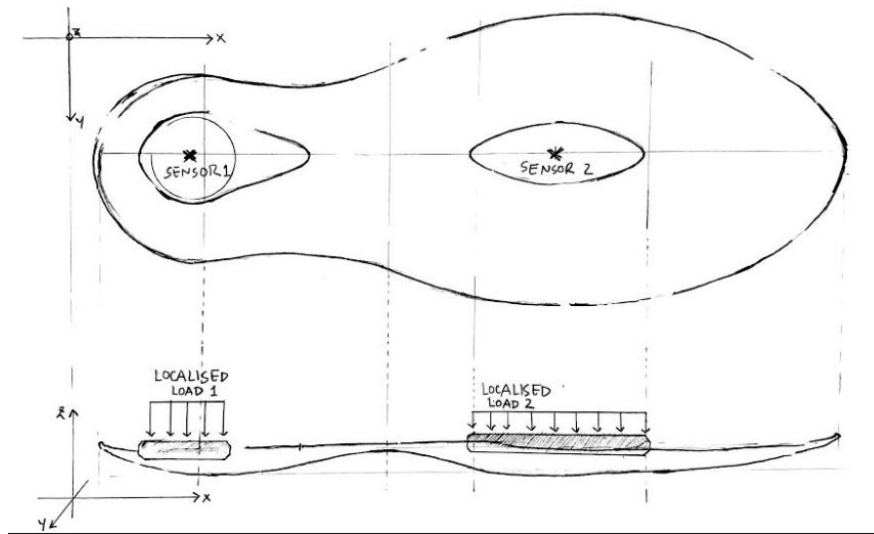


Figure 5.5: Insole with Load Sensor and Integrated Active Feedback Module

5.1.5 - Portable Electronic Pitting Device with Integrated Active Feedback Module

As mentioned previously, the current clinical standard of assessing the severity of PE is pitting. With this practice, a nurse or other healthcare practitioner indents the swollen limb using their thumb or index finger and observes the depth and rebound time of the resulting indentation. This method is highly subjective as reported levels of swelling vary from nurse to nurse, and as nurses are not readily available at home, outpatients have to self-detect this increase in fluid retention by tracking their weights daily.

A portable electronic pitting device with an integrated active feedback module is thus proposed. Figure 5.6 below illustrates the concept. The device would be readily available to outpatients but would require the patient for operation.

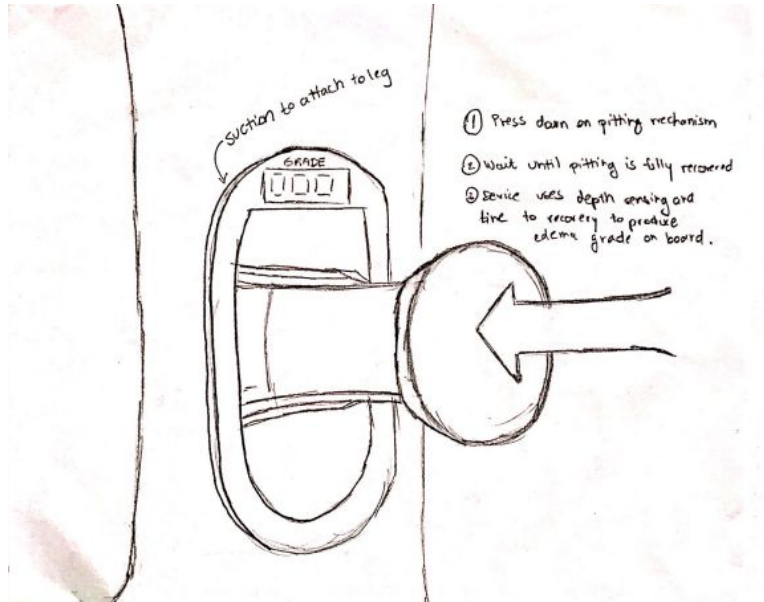


Figure 5.6: Portable Electronic Pitting Device with Integrated Active Feedback Module

The indentation mechanism would be automated using a powered linear actuator, and measurements of indentation depth would be gathered by a displacement sensor built into the device. The measurements would be collected and processed by a microprocessor, also within the device, which would in turn output a figure corresponding to the severity of the PE. The figure output will lie within the 0 to 4+ range currently used in pitting. Table 5.1 below shows the scale.

Table 5.1: Conventional Edema Scale

Edema Scale (Graded on a scale of 1+ to 4+)	
Grade	Physical Characteristics
1+	Slight pitting, no visible change in the shape of the extremity; depth of indentation 0-1/4" (<6 mm); disappears rapidly
2+	No marked change in the shape of the extremity; depth of indentation 1/4 -1/2" (6-12 mm); disappears in 10 to 15 seconds
3+	Noticeably deep pitting, swollen extremity; depth of pitting 1/2-1" (1-2.5 cm); duration 1 to 2 minutes
4+	Very swollen, distorted extremity; depth of pitting > 1" (>2.5 cm); duration 2 to 5 minutes

By employing electronics in place of visual observation, the device eliminates the subjectivity of measurements due to human error which is a major setback with current pitting practices. However, a low patient compliance is anticipated due the heavy reliance on the patient for operation.

5.2 - Down Selection

The down selection process consisted of identifying the most important quantitative and qualitative characteristics of the desired device, weighting each characteristic, and assigning corresponding characteristic values for each proposed solution on a scale of 1 to 10, as shown in Table 5.2 below.

Table 5.2: Down Selection

	Ease of Use to End User	Ease of Testing	Manufacturability	Cost to End User	Reliability of Measurements	Total
Weight	0.25	0.25	0.15	0.05	0.3	1
Ankle Strap	6.5	7	10	5	9.5	7.795
Sock w/ Stretch Sensors	8.5	6.5	9	4	10	8.3
Sock w/ Embedded Nanoparticles	6	5.5	1	2	2	3.725
Insole w/ Load Sensors	10	9	4	8	4	6.95
Portable Electronic Pitting Device	4	5	6	5	6	5.2

The first characteristic was *Ease of Use to the End User*. This characteristic is directly related to *Compliance*. A wearable device increases the likelihood of consistent use by the patient which consequently increases the effectiveness of remote monitoring. The proposed insole solution requires minimal input from the patient, i.e., placing the insole into the shoe, thus excelling this category. The sock with stretch sensors, as well as that embedded with nanoparticles sock also excel in this category. However, the sock embedded with nanoparticles employs a passive feedback mechanism in that measurements of changes in leg circumference/volume are extracted from passively observing color change and cross referencing the color change with a corresponding value of the level of PE. Because of this, the patient would require a chart for referencing, and/or a mobile app that would interpret the color change and report the progress of the PE to a physician, which effectively lowers its ease of use score. Lastly, both the ankle strap and portable electronic pitting device would require the user to take measurements of PE on roughly the exact same

position on the leg each time to ensure consistency of measurement, a requirement that inhibits ease of use.

The second category was *Ease of Prototype Testing*. Given the bureaucracy involved in the testing of medical devices, the ability to test prototypes without human subjects is very important. The socks with stretch sensors and embedded nanoparticles, the ankle strap, and the portable electronic pitting device all require an expanding leg apparatus with edematous tissue properties to simulate a CHF patient's leg. However, the proposed sock embedded with nanoparticles would require further extensive testing due to limited available research on the subject, and novelty of the technology. Tests for the insole would be fairly simple, as these would just require volunteers to place the insoles in their shoes for a day or so in order to test for measurement accuracy and for calibration purposes.

Another important characteristic of the design is *Manufacturability*. The proposed sock with embedded nanoparticles would be difficult to manufacture due to undue research and experimentation in the topic, as well as the costly nature of working with nanostructures. For the proposed insole design, the conceivability of the electronics module would be difficult since there is limited space within the shoe.

Reliability of Measurements had the highest weight in the down selection process. This would determine the precision and accuracy of the device. As mentioned above, a device that measures a change in diameter at 7 cm above the malleolus would be very effective for tracking edema. Therefore, the anklet performed very well in this category. The sock with stretch sensors allows for this measurement. The nanoparticle color change is highly subjective as it would require the observer to qualitatively compare the color of the fabric to a chart. Furthermore, the level of achievable accuracy in such a practice is unknown.

Furthermore, after consulting with Dr. Cacchione, it became apparent that the proposed insole solution would be highly prone to reporting false positives due to the other different factors upon which body weight is dependent. That is, the insole will frequently measure and report changes in weight that are not a consequence of the progression of PE. Of these factors, one of particular importance is the patient's eating habits; for instance, if a CHF patient consumes meals high in salt or sodium, their body water retention could significantly increase overnight. Consequently, the insole would correctly report an increase in weight, although the increase is not due to the progression of PE, i.e. a false positive, and this decreases the accuracy of measurements of the insole for purposes of tracking PE.

The last characteristic was *Cost to End User*. This is a reach goal and may not be in the scope of the project. The team decided to focus on making the device consistent and fully functional rather than optimizing for cost. Nevertheless, the price should not be unreasonable. The sock with embedded nanoparticles proved to be the most expensive as it utilises cutting edge technology.

5.3. Overview of Project Components

After down-selecting the different design options, the sock with integrated sensors turned out to be the optimal final system form for the proposed edema-tracking device. The implementation of such design, however, required significant validation in order to make sure that the pressure, measurement precision, and comfort constraints were carefully met. Since the sock would be worn by patients and since there are significant barriers to testing medical devices on patients, the team had to come up with additional devices that would support its testing efforts: a Leg Prototype and a Custom MTS Device

After careful consideration of the necessary validation steps and optimal system characteristics, the team concluded that a human leg would need to be modeled so that the final product (the sock) could be tested in an environment that would closely replicate its real application environment (a real edematous leg). In order to do so, the team decided to create a Leg Prototype that would have integrated force sensors for pressure testing (to make sure that the sock pressure would always find itself between P_{min} and P_{max}) and an adjustable radius in order to simulate different stages of edema and the measurement precision of the final product. The Leg Prototype will be further explored in Section 5.5

Moreover, the team set out to more closely model the leg model to a real edematous leg by adding a layer of polyethylene soaked in vegetable oil. To make sure that this layer would simulate the dynamics of edematous skin, the team created a Custom MTS Machine that would record Force versus Skin Radial Displacement graphs. These graphs were essential in deriving the viscoelastic properties of the polyethylene layer, which could then be compared with different values for real edematous legs. The Custom MTS Machine will be further explored in Section 5.4.

To sum up, there are three large components to this project:

- The Sock (Final Product)
- The Leg Prototype (auxiliary testing device)
- Custom MTS Machine (auxiliary testing device)

This report will now dive deep into the design and engineering details for each of these.

5.4. Custom MTS Machine

5.4.1 Overview

The custom built MTS machine was designed for experimentation purposes to facilitate the assessment of the viscoelastic properties of edematous tissue. The MTS machine would collect force and displacement measurements as the edematous tissue was indented. These measurements would then be used to numerically determine the viscoelastic properties of edematous tissue. In effect, developing a better understanding of the viscoelastic properties of edematous tissue requires knowledge of how edematous tissue mechanically responds to applied physical loads, and this knowledge would inform the design of the edematous leg prototype.

The machine includes an anterior that comprises a force sensor and a displacement sensor, and a posterior that comprises a powered linear actuator and an electronics module for collecting and processing signals from the sensors. The first embodiment of the machine is illustrated in Figure 5.7 below.

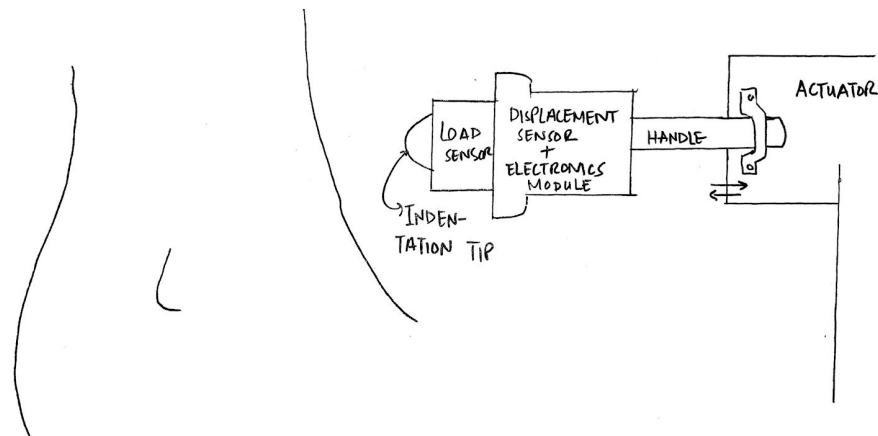


Figure 5.7: Custom MTS Machine Concept Drawing

Employing an actuator in place of a human operator eliminates the associated human error. Furthermore, it maximises consistency in data collection which positively impacts the reliability of the collected data. To successfully build the pitting device, high precision force and displacement sensors are required as the forces and displacement quantities associated with pitting edematous tissue are within the low end. Accordingly, the availability of both a displacement sensor[50] capable of appropriate resolution for a range of displacement of $0 \rightarrow 8$ mm, and a force sensor[51] with a force range of $0 \rightarrow 3$ lbs, as well as a linear actuator[52] has been confirmed.

5.4.2 Manufacturing of Final System Form

Load Cell Calibration

The load cell to be used in the MTS machine had to be calibrated before incorporating it into the final system design. This will allow the team to have a direct relationship between the digital output received from the Arduino and the corresponding force being applied onto the load cell. The calibration was performed by using cylindrical disk weights of 200 grams each. Starting off with a single weight of 200g, single weights were added incrementally until reaching a total weight of 1000g and, therefore, five measurements. At each increment the Arduino digital output change from baseline was measured and recorded. Following this, a linear regression was calculated between the applied force, in Newtons, and the resulting digital output (see Figure 5.8 for resulting calibration). This linear relationship is ultimately what was used to calculate the force readings acquired from the MTS Machine.

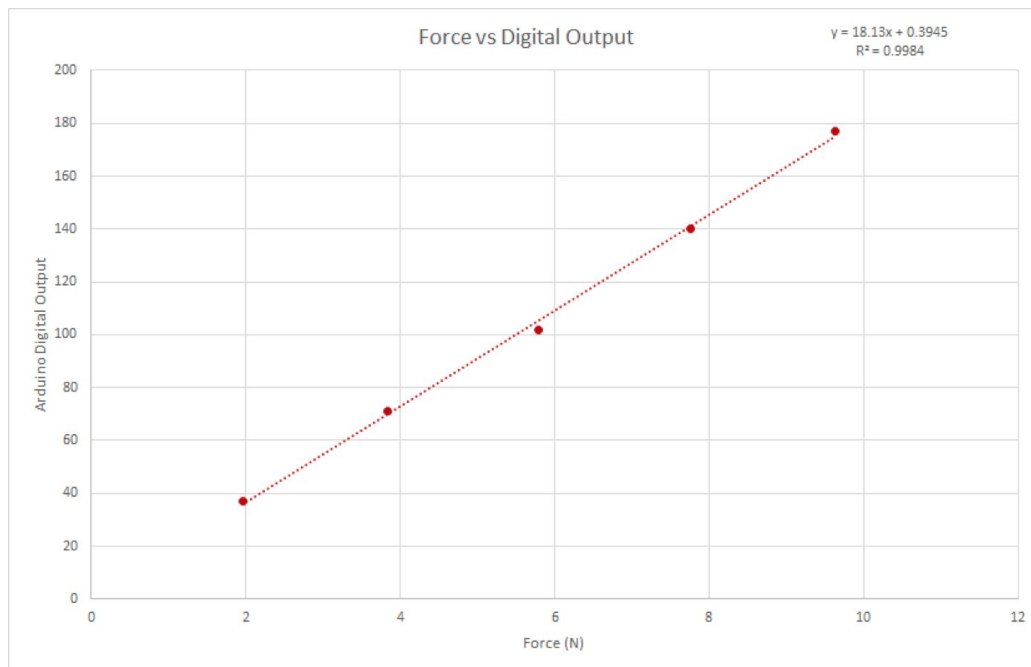


Figure 5.8: MTS Machine Load Cell Calibration

Displacement Sensor Calibration

The displacement sensor (slide potentiometer) specifications specified that the relationship between voltage output and displacement was linear. Therefore, all that was needed to calibrate the sensor was its voltage output at its maximum displacement (maximum resistance) and at its minimum displacement (minimum resistance). These two values were experimentally obtained. Given these

two points and the assumption that the relationship was linear, a linear regression was fit onto the points and the calibration equation was obtained.

Circuit Diagram

The final circuit implemented in the MTS Machine implements 5 main components: an Arduino Uno, a L293 quadruple half-H driver, a motor driver, a linear actuator, and a 9V battery. The 9V battery was used to power the motor driver and the motor driver in turn was able to send an input to the H-bridge to then be sent to the linear actuator. The Arduino was used to power the H-bridge and read in the data from the displacement sensor and load cell. An overview of this schematic can be seen in Figure 5.9.

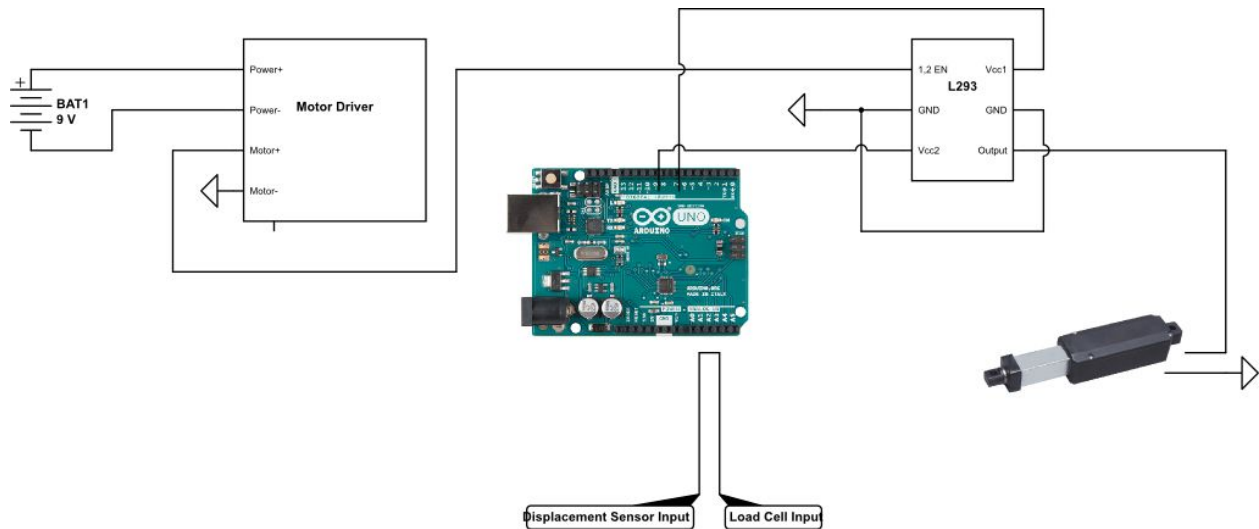


Figure 5.9: MTS Machine Circuit Diagram

Script

Using the Arduino IDE, a script was uploaded to the Arduino Uno mounted on the Custom MTS Machine to control the movement of the linear actuator, detect changes in displacement from the displacement sensor, and collect Force measurements from the load cell.

First, the script encoded a method to initiate its outputs, which are voltage being sent out to power the linear actuator, load cell, and displacement sensor, and its inputs, data from the load cell and displacement sensor. In this fashion, the linear actuator was controlled to move at the speed of 5mm/s towards the material to be pitted, while force and displacement profiles were collected. In order to satisfy our stakeholder's safety concerns for IRB approval, a maximum applied force of 10N was set as a threshold to terminate the pitting, encoded by an "if statement". Previously generated calibration curve equations were included in the code during data collection, allowing for translation between voltage to force on the load cell and voltage to distance for the displacement sensor. Lastly, the script allowed for data to be displayed on Arduino's Serial Plotter/Monitor, where data was then transferred into Excel for post-processing.

In its final iteration, the script performed the following steps on the pitting device:

1. Move the linear actuator at 5 mm/s towards the material to be pitted
2. Collect Force (N) from the load cell and Displacement (mm) from the displacement sensor
 - a. Terminate if force exceeds 10N and return actuator to initial position
3. Extend pit tip to actuator limit of 20mm, hold for 1 second, and return actuator to its original position while still collecting Force and Displacement data to see the response of a material to pitting.
4. Display data on Serial Monitor for transferring and post-processing

Note that the script is included in the Appendix and all code is properly commented with labelled digital and analog pins as well as suitable variable names for facilitated customization of pitting procedure.

5.4.3 Final Design

Figures 5.10 and 5.11 below illustrate the final design for the Custom MTS Machine.

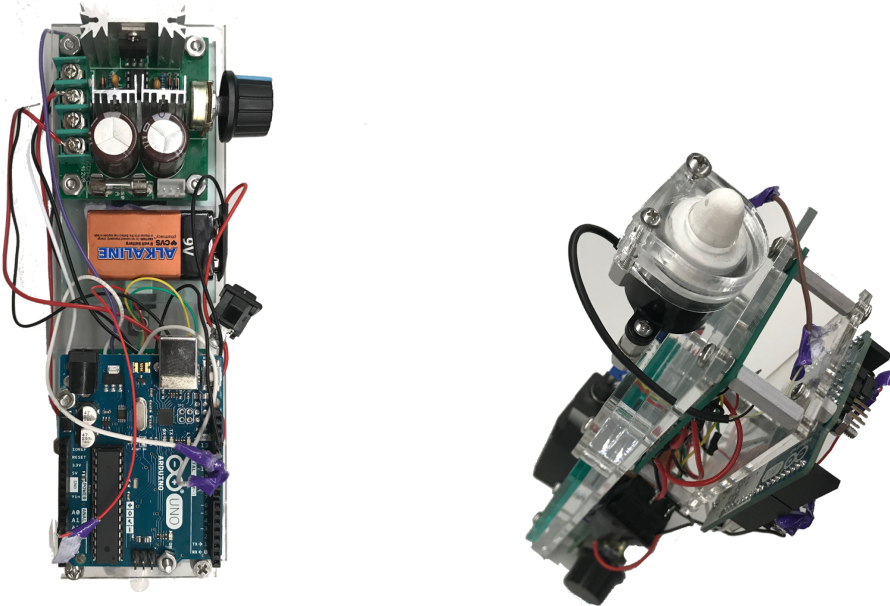


Figure 5.10: Top and Diagonal Views of Final Custom MTS Machine Design

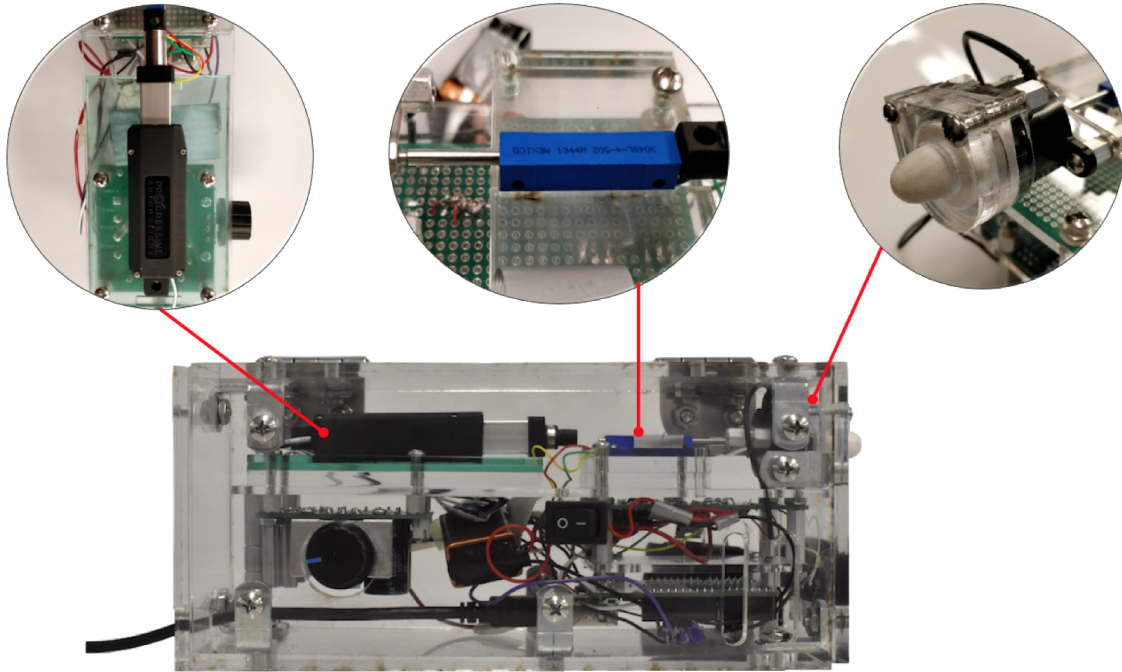


Figure 5.11: Lateral and Component Views of Cased Custom MTS Machine (Components From Left to Right; Linear Actuator, Displacement Sensor, Load Sensor)

5.5. Leg Model

5.5.1 - Ideation

In order to implement the leg prototype, the team took an iterative approach to design down-selection. It initially ideated and implemented the most simple and straightforward design that would, in theory, be able to meet every optimal system characteristic outlined in Section 4 - pressure, measurement resolution, and radius range constraints. The first design consisted of a Telescoping Rods System of straight plates and the second - and most advanced - design consisted of a Radially-Expanding System of curved plates.

Telescoping Rods System

The first design (Telescoping Rods System) consisted of four radially expanding straight faces (see Figure 5.12 for design). The face were placed at the opposite ends of two horizontally perpendicular axis and could be adjusted in order to simulate different stages of leg expansion, thus edema stages.

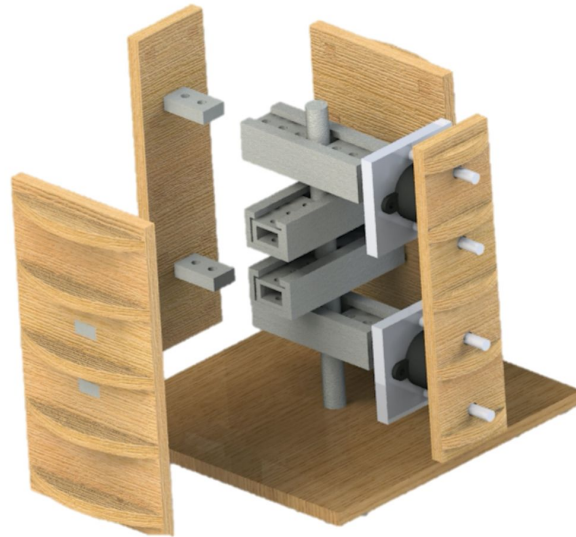


Figure 5.12: Telescoping Rods System

The system's main features were:

- **Discrete adjustment of face radii:** each face had three different radius settings - small, medium, and large - as is evidenced by the screw slots on the arms of the leg in Figure 5.12.
- **Different widths for Lateral and Front/Back Plates:** By making the lateral plates wider than the front and back plates, the team set out to model a leg with elliptical cross-section, which better approximates the cross-section of a real leg at 7cm above the medial malleolus. In this way, the team could also guarantee that the maximum force applied to the leg would be concentrated on the longest axis (Front/back axis), which would make the measurement of the highest force easier and more accurate.
- **Force measurement on one of the four plates:** Two load cells were connected to one of the four faces, which was left unattached to the main structure to avoid interference in the force measurements. The force measurement plate was chosen to be the plate that would always have the largest radius (modeling the tibia protrusion in the front of human legs). The team made the crucial assumption that, since this face would have the larger radius, it would also feel the highest force from the sock. This way, the team would be able to accurately capture the maximum pressure being applied on the leg model (P_{max})

Radially-Expanding System

The second design consisted of a Radially-Expanding System of five arches whose radii could be adjusted in a continuous range of values. The five faces would be uniformly distributed throughout a circumference (tangentially spaced out by 72 degrees) and could be adjusted by a gear mechanism

that would push the faces outward when rotated clockwise and pull them inwards when rotated counterclockwise (see Figure 5.13 for design).

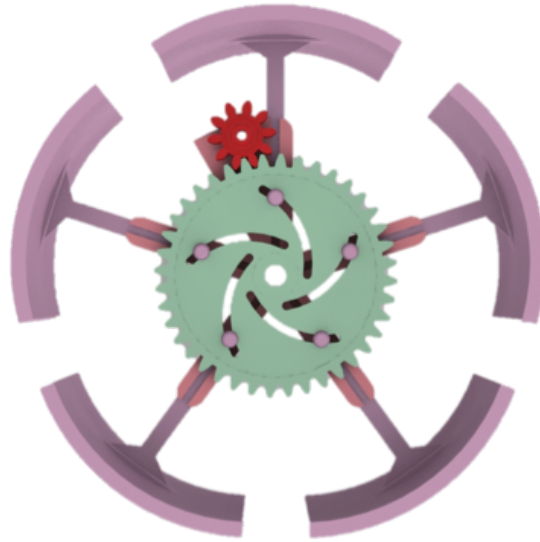


Figure 5.13: Radially-Expanding System Design

The system's main features were:

- **Continuous adjustment of face radii:** differently from the Telescoping Rods System, the Radially-Expanding System could be adjust in a continuous way. This was due to the use of a gear system that would drive the expansion of the arms, as mentioned above. The other main difference from the Telescoping Rods System was that the radius of the faces could not be adjusted individually. The system operated in an integrated way.
- **User-friendly mechanisms to adjust and “lock” radius:** The main priority of the second design was to facilitate testing at different radii. For this reason, it was imperative that the team design a way to quickly change the radius of the leg. A rack-and-pinion system was devised to transform the rack translational motion into the shaft rotational motion, which would in turn drive the rotation of the main gear that was responsible for pushing and pulling the faces outwards and inwards.
- **Identical curved faces:** differently from the Telescoping Rods System, the faces in the Radially-Expanding System had the same dimensions. This limited the cross-section of the leg model to a circular shape, but allowed the team to relax some assumptions with respect to the location of the maximum force applied to the leg (see next feature for main reason).

- **Flat Force Sensors integrated on each face:** instead of placing two load cells on the face that would presumably feel the strongest compression from the sock, the team decided to track the force/pressure distribution on 10 different areas of the leg (5 x 2 curved plates).

5.5.2 Design Iteration

Telescoping Rods System

After implementing the first design (see Figure 5.14 for prototype), the team set out to evaluate its performance. In order to do so, the team inserted the entire device inside a sock that would compress the faces of the prototype and proceeded to record force readings at different leg diameters. While the team was able to acquire data with this procedure, the testing routine brought out the flaws in the design of the Telescoping Rods System. More specifically:

- **The force readings for each load cell were significantly different:** the team expected the two load cells to output very similar measurements but there was a clear discrepancy between the readings for both sensors. While this could be in part due to the sock's pressure gradient, the team concluded that there was a chance that such discrepancy came from a design failure.
- **The data was considerably noisy:** As evidenced by Figure 5.15, although there is an upward trend on the force as the diameter of the prototype increases, the force readings are extremely volatile, which points to a suboptimal precision of the model's force measurements.
- **The testing procedure was extremely cumbersome:** it took too much effort for the team to change the settings of the leg model (diameter), which is why the team was only able to record 4 different radius settings during testing procedures (see Figure 5.15).

Other flaws from this design include:

- **Maximum Force Assumption:** This design assumes that the maximum force will always be recorded at the face that contains the load cells. This seemed to be a fair assumption given the elliptical face of the leg prototype, but was still an assumption at the end of the day. This fact decreased the reliability of test results and was one of the main reasons the team decided to iterate on the Leg Prototype Design.
- **Wobbly faces (too many interfaces):** Each face was connected to a laser-cut piece of MDF that was attached to a piece of 3D printed material, which was itself attached to the core of the structure. Given the several interfaces between each element, the Leg Prototype was not sturdy enough to generate reliable test results.

- Radius range was not respected:** the minimum radius of our single prototype was too large given the optimal range defined at the ideation stage. It turned out that the Telescoping Rods System design was unsuitable to recreate the minimum, non-edematous leg diameter, since the Telescoping Rods were composed of too many elements that each occupied significant space in the structure. Unfortunately, it would have been infeasible to manufacture the prototype at a smaller scale as it would have been structurally weak and could possibly fail in different testing scenarios.

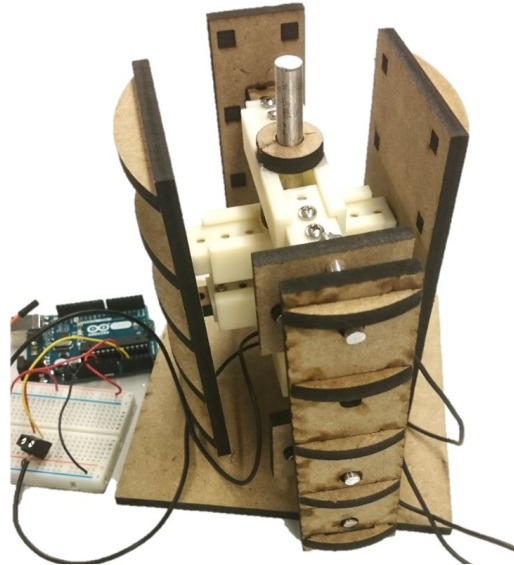


Figure 5.14: Telescoping Rods System Prototype

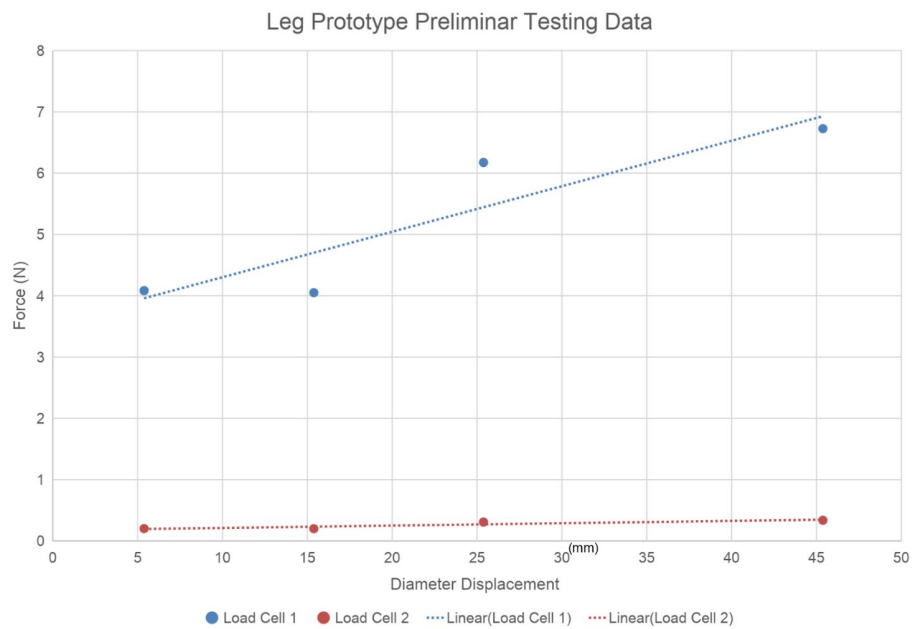


Figure 5.15: Preliminary Test Data for Telescoping Rods System Prototype

The testing procedure showed that the Telescoping Rods System would be unable to accurately report the maximum force readings on the leg. For this reason, the team decided to iterate on the initial design to build the more advanced, Radially-Expanding System, as the subsequent design iteration.

5.5.3 Final System Form

The Final System Form of the Leg Model was an amalgamation of (1) radially expanding rod and a rack/pinion for moving said rods, (2) an array of 1.5" Square Force Sensing Resistors placed on the outer circumference of the telescoping rods, and (3) laminating of the outer circumference of the leg model with artificial edematous tissue. Along with these three crucial components, a base made from laser cut MDF was designed in order to fasten the leg model, the Arduinos which would read data from the Force Sensors, and make measuring changes in diameter more salient with a graduated ruler etched onto its surface. Finally, two separate leg models were created in order to capture the full range of radii from smallest adult ankle size without edema (3.5cm) to largest adult ankle size with edema (7.3cm). Figures 5.16 to 5.20 outlines the team's nomenclature for each sub component to facilitate comprehensibility of protocol for manufacturing.

(1) Radially Expanding Rods

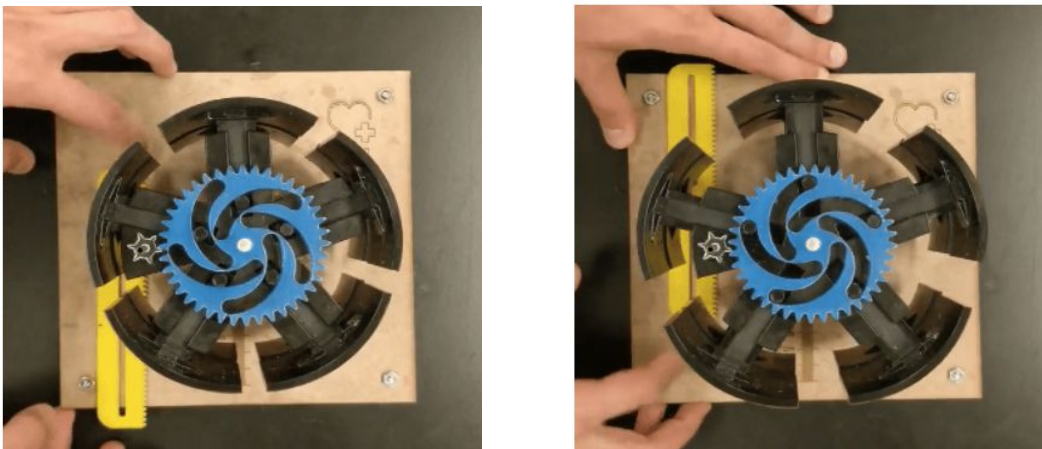


Figure 5.16: Radially Telescoping Rods. Five rods stacked in two layers allow for symmetric radial expansion when sliding the yellow rack upwards

(2) Force Sensor Array

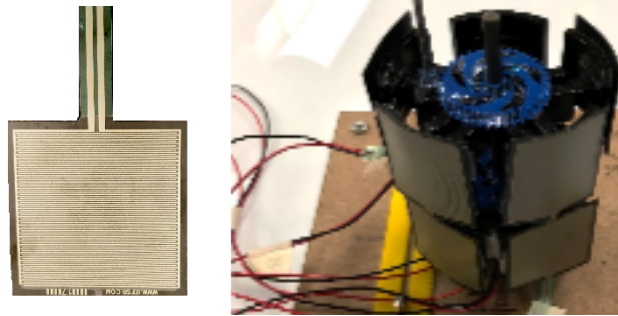


Figure 5.17: Array of Force Sensors. 10 Force Sensors per Leg Model were adhered to the outside of the telescoping rods to detect pressure changes with a resolution of $0.196\text{N}/\text{cm}^2$

(3) Lining of Artificial Edematous Tissue to Model Human Tissue Response Behavior



Figure 5.18: Medical Grade Edema Testing Kits Used to Line Leg Model Outer Circumference. Test kits would be used for long term creep tests for a more accurate tracking of ankle circumference by considering tissue response mechanics

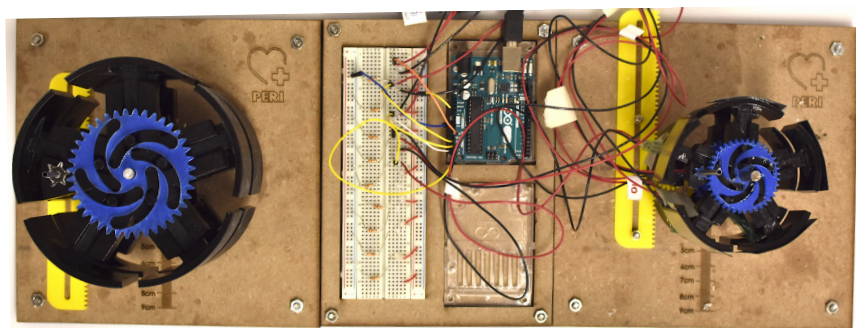


Figure 5.19: Bird's Eye View of Final Leg Models Side by Side. Small Leg Model connected to Arduino. Base contains slots for extra Arduino for force sensors to be attached to Large Leg Model.

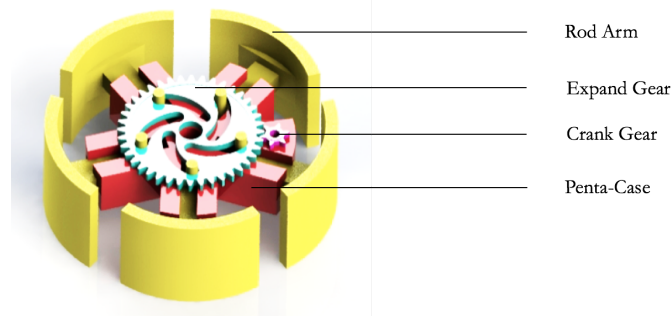


Figure 5.20: Nomenclature of Subcomponents of Leg Model. Leg Model Key Components and how they will be referenced for the remaining portion of this section

5.5.4 Manufacturing of Final System Form

To create this leg model, access to 3-D printers, machining tools, and laser cutters is required. The process involves combining 3-D printed parts — telescoping rod arms and penta-case — parts that are laser cut — gears and rack – and parts that are manually machined —shafts. Using the computer aided design software SolidWorks, all parts were modelled to our design specifications and can be seen in the Appendix.

3-D Printing

Through the Additive Manufacturing Laboratory at the University of Pennsylvania, the penta-case and rod arms were printed using the Objet30 printer with resolution at 28 microns in VeroBlack Opaque Material, an acrylic-based photopolymer. The first time the parts were received after printing, the team recognized a design flaw with the size of the rod arms cross-sectional area. Its tight fit interfered with sliding of the arms in the penta-case slots, as seen in Figure 5.21, and thus a new design was proposed where much thicker rod arms and more spacious penta-case slots were used. This design proved functional and smooth in sliding.

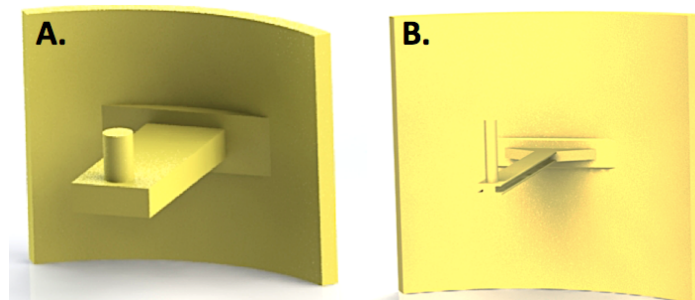


Figure 5.21: Comparison between (A) final iteration and (B) first attempt at creating a rod arm.

Laser Cutting

The gears were laser cut in quarter inch acrylic according to the drawing file in Figure 5.20. Recall that the smaller gear is attached to the cranking shaft that is turned via the movement of the yellow rack whilst the larger gear is used to push the rod arms outwards as it spins counterclockwise. The yellow rack, shaft collars, and yellow gear seen in Figure 5.22 that are used to spin the cranking shaft were laser cut using eighth inch acrylic. Finally, the base of the design was cut using quarter inch MDF, with holes of radius 0.25 inches for the main shaft and slider fasteners as seen in Figure 5.22.

Assembly

The following step by step protocol was used to combine all parts into a final Leg Model. It is worth reiterating that assembly for the small and large leg models are identical, only the size of parts are different.

1. Collect materials for assembly: total of 10 rod arms, 2 main gears, 2 small gears, 1 racks and pinion, MDF base, 2 shafts, 2 shaft collars, and 2 penta-cases.
 - a. Additional Material necessar includes Super Glue, File, and WD-40.
2. Verify that Rod Arms slide smoothly along penta-case slots. File if necessary the inside of the slots and the outside of the rod arms and lightly apply WD-40 to further reduce sliding friction.
3. Press-fit Main Shaft onto base and slide first shaft collar down main shaft, now erected, until it lies 5 cm above base surface. Apply Super Glue to collar interior for adhesion to main shaft.
4. Slide penta-case down main shaft and align slot for cranking-shaft on the case with slot on the base. Slide the cranking-shaft through the case onto the base. Secure the penta-case onto top of shaft collar using Super Glue.
5. Slide rod arms into slots on penta-case and slide Main Gear down main shaft such that pins from each rod arm fit evenly inside the slots of the Main Gear itself. Attach the small gear through the cranking-shaft such that it lies in the same plane as the Main Gear. Secure it in place using Super Glue.
6. Place a second shaft collar down the main shaft such that it lies 12 cm above the base and repeat steps 4-5.
7. Cranking shaft should now be able to twist and expand/contract the leg. Attach pinion to bottom of the cranking shaft and place rack such that its fastening pins fit into its slot allowing for linear motion. The rack stoppers can be used here to keep radius at any desired value between the minimum and maximum of its respective leg model.

Once assembled, the design takes on the form seen in Figure 5.22.

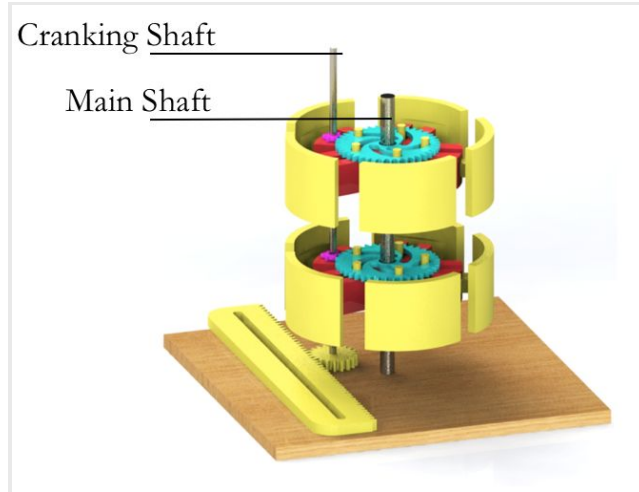


Figure 5.22: Rendering of Finalized Assembled Leg Model. Before placing force sensors on rod's outer faces

Sensors

The 15mmx15mm square force sensing resistor was chosen because of its resolution of 19.6N/cm² as well as its shape of . The design of the outer face of each telescoping rod fit exactly one force sensing resistor. Each force sensor was calibrated individually, translating output voltage from a simple voltage divider circuit array, to pressure, seen in Figure 2.23 below. After calibrations were performed, a standard deviation of roughly 0.11 was calculated for the slope and 7.87 for the intercept. This led to a 95% confidence interval of the calibration slope lying between 4.79 and 4.31. Translating these slopes to a pressure change, it is calculated that there is an uncertainty of ±0.265mmHg (or 0.529 if considering cloud around point) of reading around any data point collected, which was deemed acceptable. The intuition behind this was that as long as the maximum pressure obtained with the final sock plus this uncertainty remained below the target pressure, the constraint would be met. Furthermore, this value of ±0.265mmHg is lower bounded by the coefficient of the exponential function it was modelled after, at 0.5209. Thus, uncertainty achieved was 1.7% away from no error (see Table 1 and refer to Section 5.6.4)

Table 5.3: Force Sensor Calibration Uncertainty Breakdown

Average Slope(AnalogRead/g)	4.5584
Slope Standard Deviation	0.1190
Slope Variance	0.0141
Slope Confidence Interval	4.7962 — 4.3199
Uncertainty ±(g)	0.1044
Uncertainty ±(AnalogRead)	±0.4762
Uncertainty ±mmHg Translation	±0.5289

A Matlab script was developed to display pressure profiles at 10 points around the leg. It is worth noting here that the average intercept, roughly -23.52, corresponds to the minimum detectable

pressure of the Force Sensor at 20g, or 19.8 AnalogRead values . Thus, the intercept was off by 15.9% relative to the expected value from the product’s datasheet and could come from variability between force sensors.

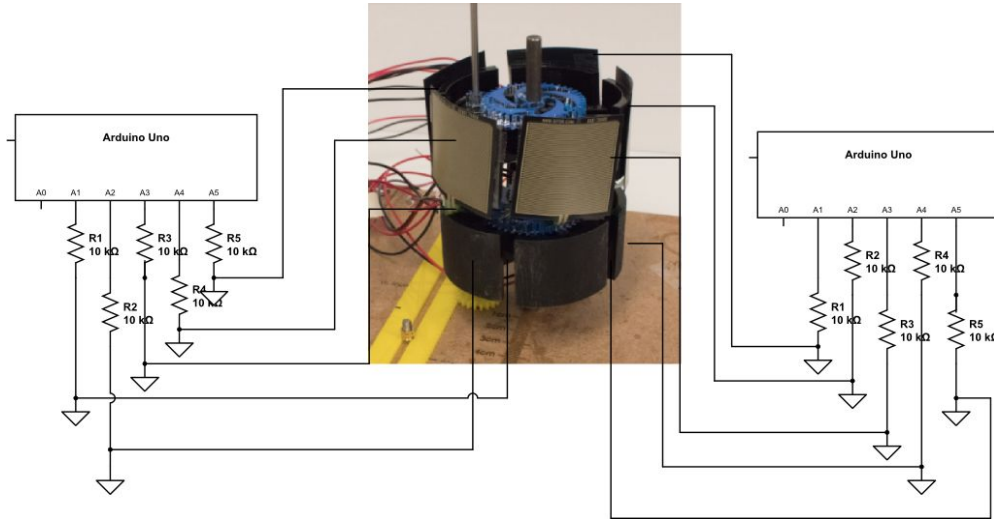


Figure 5.23: Circuit array of voltage dividers leading to 10 force sensors being read by MATLAB script

To attach the array of sensors, double sided tape was used to secure each sensor onto the face of the telescoping rods. To ensure repeatable readings from the force sensors, they were fastened in a bent shape as to fit the curvature of the telescoping rod such that pressure applied by the sock would not deform the sensor and thus affect the sensor readings due to sensor tampering rather than pressure being applied.

A Matlab script was devised to read in data from these force sensors and display them in a user friendly manner such that live pressure feedback from each sensor is provided. Figure 5.24 shows an example of the plotting setup in Matlab. In addition to data visualization, the script facilitates saving data for future use and is included in the Appendix package. Calibration of the force sensors is included in Section 5.6.4.

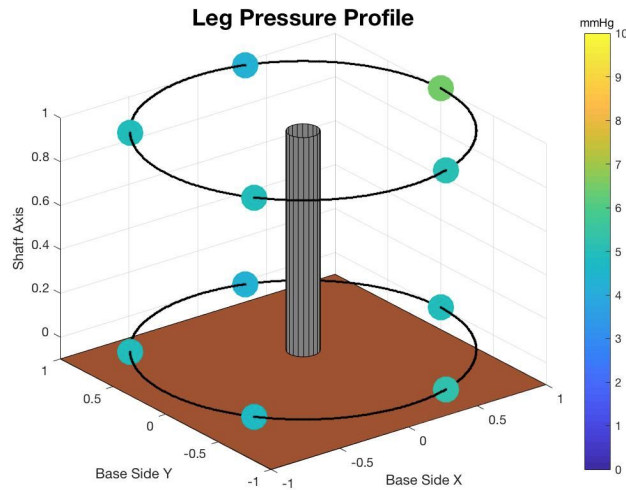


Figure 5.24: Pressure Profile example developed using MATLAB that updates in real time

Foam Study

The purpose of the foam study was to model artificial material that accurately simulates the behavior of live edematous tissue. In effect, the artificial material to be modeled would be required to possess viscoelastic properties approximately equal to those possessed by live edematous tissue, or those possessed .

The conducted literature review revealed that high density memory foam soaked in vegetable oil accurately simulates PE by varying the thickness of the soaked foam. The protocol for preparing the soaked foam was adopted from LeGare *et al.*[53] as outlined below.

Foam Preparation

1. Cut three 4" x 4" pieces of memory foam from the mattress topper. When they are initially cut from the mattress topper, their thickness is 1.25"
2. Cut one piece of memory foam into two pieces. The first piece should be 4"x4"x0.50," and the second piece should be 4"x4"x0.75." This can be done by using a band saw.
3. Cut another piece of memory foam into two pieces. The first piece should be 4"x4"x0.25," and the second piece should be 4"x4"x1."
4. Place one piece of memory foam into each of the five containers.
5. Pour vegetable oil into each container. Submerge the memory foam in the liquid, pressing out all of the air. Repeat until the memory foam is completely saturated. The foam should not float in the liquid.
6. Ensure that the top of each piece of saturated memory foam is no more than a couple of millimeters below the vegetable oil.
7. Cover each container.
8. Wait between four and six hours before testing the memory foam.

9. Immediately before testing, ensure that the memory foam is saturated.

5.5.5 Final Design

Figure 5.25 and 5.26 show a lateral and a top view of the small leg prototype without the integrated sensors, foam, and circuitry. Figure 5.27 provides an illustration of the final small leg prototype with integrated sensors and functional circuitry.

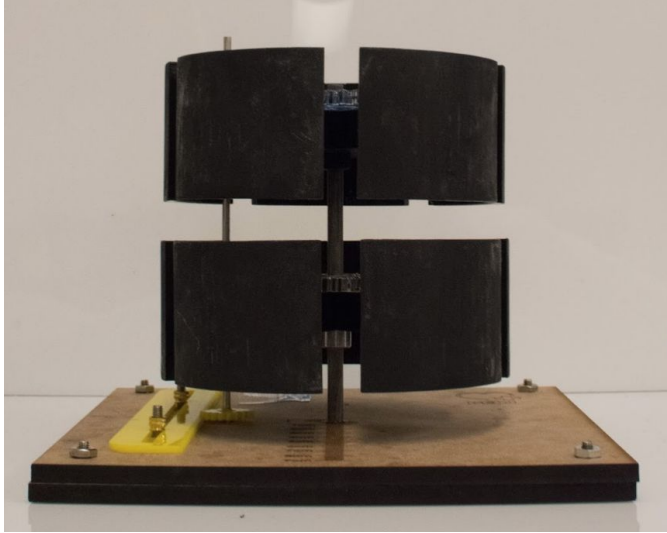


Figure 5.25 : Small Leg Prototype Lateral View

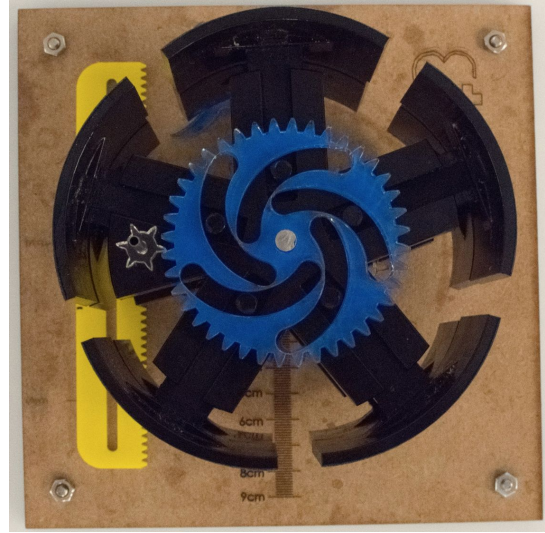


Figure 5.26: Small Leg Prototype Top View

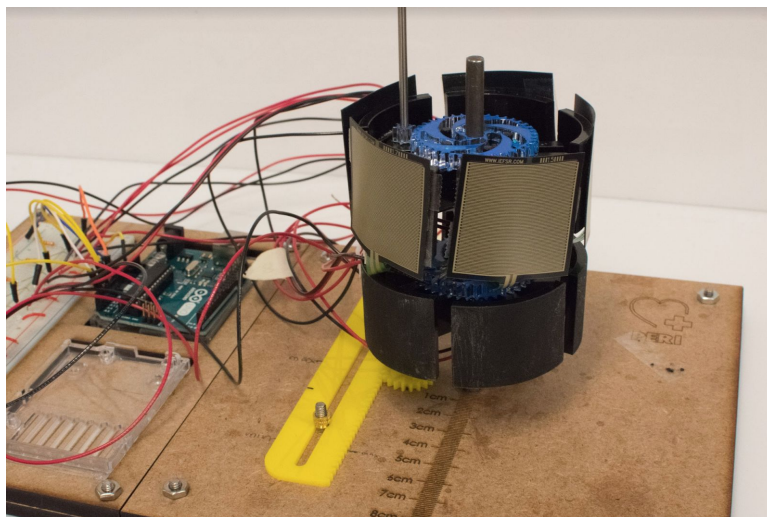


Figure 5.27: Small Leg Prototype with integrated Pressure Sensors and Circuitry

5.6. Sock

5.6.1 - Ideation

After having met with Drexel Manufacturing Lab to discuss a partnership, the team ideated the most viable technology that could be sewn onto a sock that would follow the design constraints previously established. Of the ones discussed, the team narrowed down design options to two potential methods of sock manufacturing, and as a consequence, sock design. Both can be seen below in Figure 5.28.

The first design included one single resistance band attached at 7cm above the medial malleolus, as this is the point in the leg where the curvature is no longer concave and thus is considered an equilibrium point. To further ensure that the resistance band would be placed closest to this designated area of optimal readings, stiffer material would be sewn to the bottom portion of the sock, where the foot lies. This would prevent a patient from pulling the sock above the point at 7cm above medial malleolus. Building off the stiffer material idea, the team proposed a hoop of stiffer material instead of changing the entirety of the lower portion of the sock for user comfort. At the opening of the sock, a velcro flap could case the electronics consisting of a BLE Module and a battery. These electronics and the terminals connecting to the stretch sensor would be shielded so that the socks would be washable. Lastly, conductive fabric would be sewn in the sock to send the signal from the resistance band to the electronics module.

The second iteration of this design included the same velcro and shielding capabilities, but counted on a spiral wrapping of a longer resistance band across the entirety of the leg. After having down-selected out of the possibility of including several stretch sensors so to create a volumetric profile of the leg using the Frustum Method (**see Binding Project Proposal**), the spiral wrapping method had the advantage of having a greater linear range. Because the stretch sensors undergo stress relaxation after stretching to 150% its original length, having an extremely long sensor that wraps the leg would ameliorate this shortcoming. Furthermore, instead of a velcro flap, there would be a magnetic strip to allow for closing the protective flap.

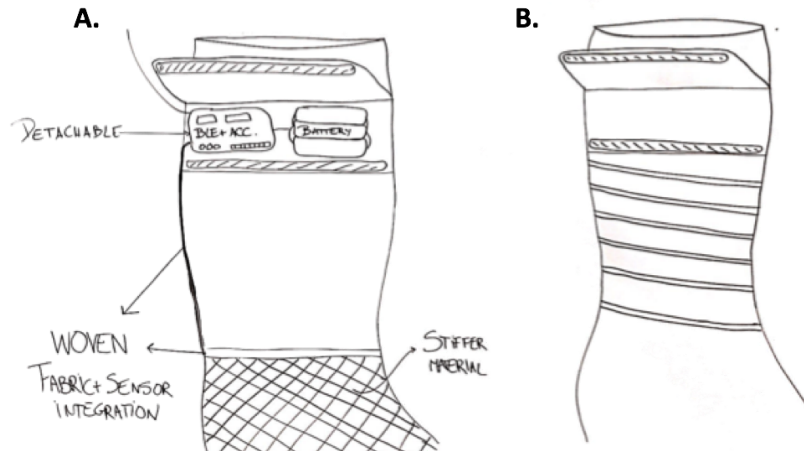


Figure 5.28: Sock Ideation. (A) First proposed solution and (B) Second Proposed Solution

5.6.2 - Down Selection

Ultimately, it was decided that the first iteration of the two sock prototypes was the optimal solution, although some components of the idea were also shared for the second idea. The criteria for this selection are listed below:

A. Stiffer Material For Repeatability of Measurement

- a. Having a stiffer material at the bottom of the sock is a crucial component of the design because it would allow users to not worry about the location of the resistance band as the only point of interaction with this component would literally be putting the sock on. Could have a degree of comfort reduced though.

B. Woven Conductive Fabric

- a. By incorporating electronic components into the sock, manufacturing would be faster and the final product more integrated such that less interactable components exist. The conductive fabric is both safe given the low current and voltage supplied by the electronics module

C. Detachable Electronics Module

- a. The module, which would be shielded by a case decided to be of silicone because of its elastic properties so that users experience the least amount of resistance and so that it could be easily cast. When deciding how to attach the module to the sock, a shielded terminal was chosen but not ideated upon because it had been a consensus among the team that a magnetic terminal be used based on the design implemented by the company Sensoria[54]. This terminal type makes it easy for the user to clip on the module as well as reducing the need to interact with it. The velcro sleeve was therefore a consequence of this decision because of the number of magnets embedded in the sock itself to connect to the module. This optimal solution does

have one shortcoming and it is in washing. For users who have metal washers or dryers, the sock magnets would attach to washer/dryer walls, making it easy to lose them and making them more susceptible to damage.

D. Single Stretch Sensor

- a. Although multiple stretch sensors seemed convincing at first, it was induced that covering a greater area of the leg made circumference readings more susceptible to noise, not to mention that literature not found on the accuracy of this type of measurement whereas 7 cm above the medial malleolus does. Furthermore, having a larger stretch sensor means that there are more points for failure.

5.6.3 - Final System Form

The final system form of the sock consisted of three main subsystems: the sock fabric, electronics and electronics module casing. The sock fabric was chosen based off desired characteristics such as pressure exertion, heat dissipation, and moisture wicking. The electronics consists of the elastic stretch sensor along with the circuitry housed in the module casing. Lastly, the electronics module casing was manufactured using liquid silicone (ECOFLEX 00-30) and a custom 3D printed mold. An overview of all the components on the final sock layout can be seen in Figure 5.44.

A block diagram of the the electronics involved can be seen in Figure 5.29, and will be explained with the PCB.

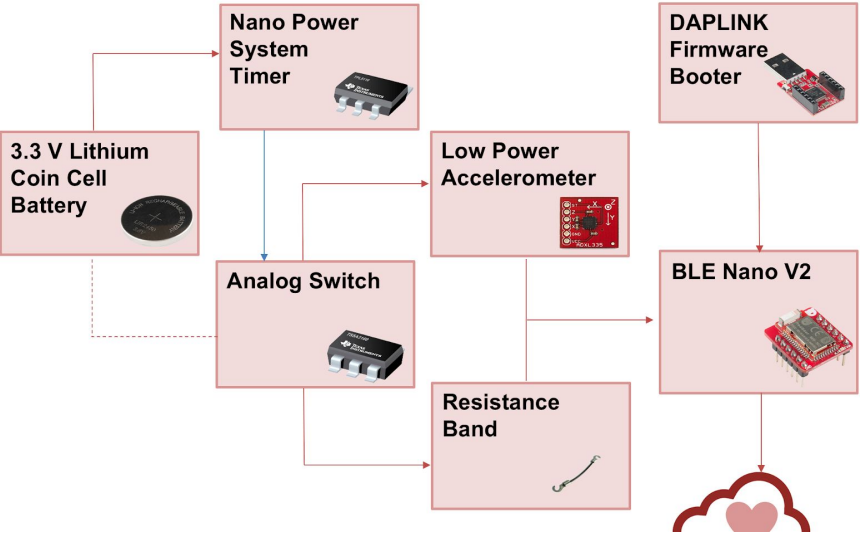


Figure 5.29: Block diagram of electronics module on sock

The team devised two iterations of the electronics module casing, a larger case to house the larger breadboard prototype, and a smaller case to house the miniaturized PCB prototype. The casing was

constructed using a custom-made 3D printed mold. The relative size of each case and the custom mold are demonstrated in Figure 5.30.

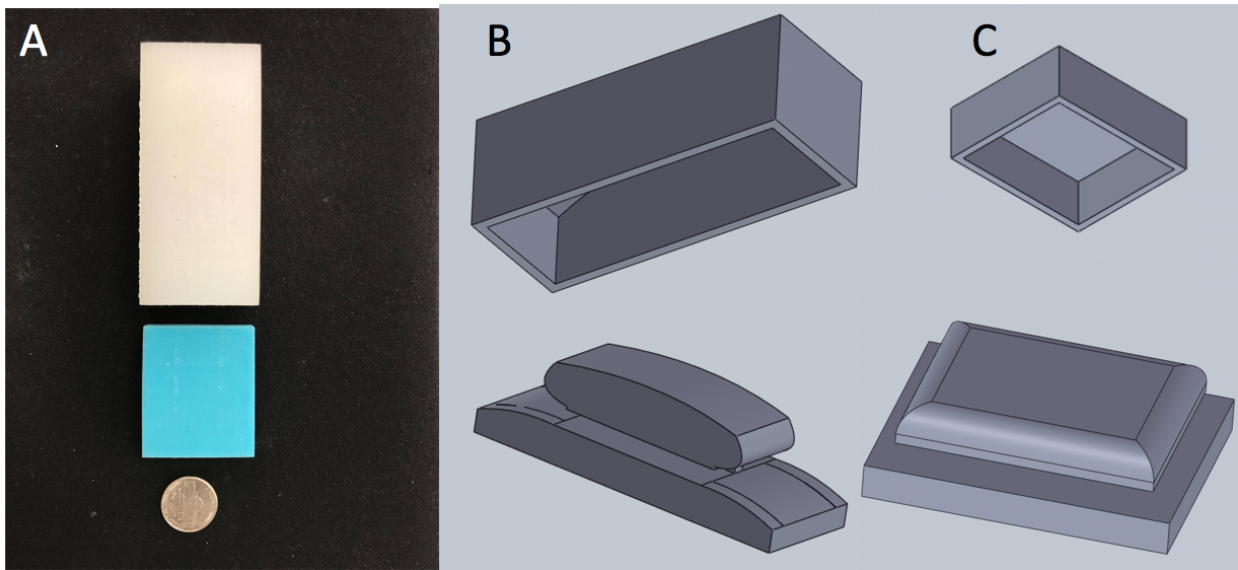


Figure 5.30: (A) Molds for Electronics Casing, nickel for scale. (B) Casing mold iteration 1, more bulky and fits more parts. (C) Casing mold iteration 2 to fit miniaturized version of PCB.

5.6.4 - Manufacturing of Final System Form

The team's initial plan was to manufacture the sock at Drexel's Shima Seiki Haute Technology Laboratory. After meeting with the laboratory's director at the end of the fall semester, the team received encouraging news that it would be able to utilise the Lab's machinery to sew a customized sock integrated with washable sensors from scratch. However, as the Spring semester progressed, it became clear that the collaboration process would be extremely cumbersome since both sides had to sign NDAs and receive clearing from executive branches of both schools. Although something could have likely been worked out in the medium to long term, the team did not have time to go through the entire procedure in the Spring semester. After it became clear that outsourcing the manufacturing of a customized sock to a third-party would also be infeasible given the time and budget constraints, the team decided to manufacture the sock in-house.

In order to manufacture the sock, the team had to select the right materials that would make the sock compliant with the system characteristics outlined in Section 4. More specifically, the sock should pass the pressure range requirements, precisely measure the change in leg diameter 7cm above the medial malleolus, and pass different comfortability tests, which will be explored in subsequent sections of this report. In order to do so, the team ordered 12 different sock models with different pressure specifications and sizes, including zero-pressure diabetic socks, in order to

compare models and check which one would best fit the product requirements previously outlined in this report.

Sock Pressure Tests

One of the tests that the team did in order to down-select the ideal material for the sock was the Maximum Pressure Test. The Maximum Pressure Test consisted of placing 12 different sock models of the same size (Large), carefully pre-selected, on the leg prototype and measuring the resulting radial force that each applied to the prototype at the maximum radius. This procedure was repeated 3 times for each sock and the average was recorded as the final measurement. Test results can be seen on Figure 5.31 and raw data can be seen on Table 5.4.

In order to clearly distinguish between the benefits of zero-compression socks (Aetrex 1 and 2, Euros, Sockwell, and Smartknit) and compression socks (Savoiken 1 and 2, Compressionz, Doc Ortho, Finefit 1 and 2) the team included compression socks in the tests. These ranged from 20-30 mmHg (Savoiken), 15-20 mmHg (Finefit), and 10-15 mmHg (Compressionz, Doc Ortho). With this procedure, the team made sure that the measurements taken for zero compression socks could be benchmarked against known pressure ranges for each sock. Any uncertainty coming from imprecision in the leg model measurements was eliminated since the team was able to use these benchmarks and generate a calibration curve based on manufacturer accuracy of pressure, known to be. Figure 5.31 below depicts said calibration curve which follows an unconventional line of best fit, but was fitted to allow for predictions between discrete data points of socks with known pressures. This extrapolation was deemed suitable because of the large number of socks with known pressures used, ranging from 0 mmHg to 35mmHg.

Based on test results, Euros was the best-performing sock in terms of Maximum Pressure applied to the leg, followed closely by Aetrex 1 and 2, Smartknit, and Sockwell. Doc Ortho, Compressionz, Finefit 1 and 2, and Savoiken 1 and 2 were eliminated since their maximum pressure on the leg prototype exceed the predetermined P_{max} value. After conducting the Maximum Pressure Test, the team proceeded to implement the Moisture Wicking Test and Heat dissipation Test to further down-select socks based on their comfort level to the end user.

Table 5.4: Maximum Pressure Test Results

Sock	Average Maximum Pressure Observed
Savoiken 1	22.4 mmHg
Savoiken 2	25.6 mmHg
Compressionz	9.8 mmHg
Aetrex 1	2.8 mmHg
Doc Ortho	11.3 mmHg
Aetrex 2	3.9 mmHg
Finefit 1	17.4 mmHg
Finefit 2	18.2 mmHg
Euros	2.2 mmHg
Sockwell	4.7 mmHg
Smartknit	2.7 mmHg
Venactive	6.4 mmHg

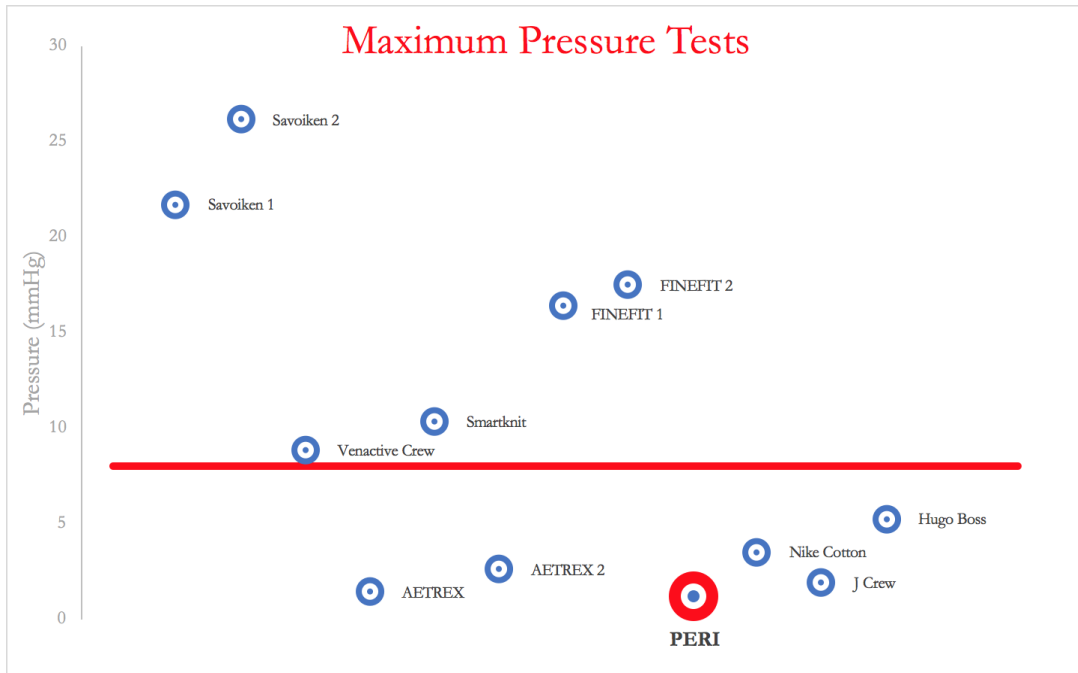


Figure 5.31: Maximum Pressure Test Results

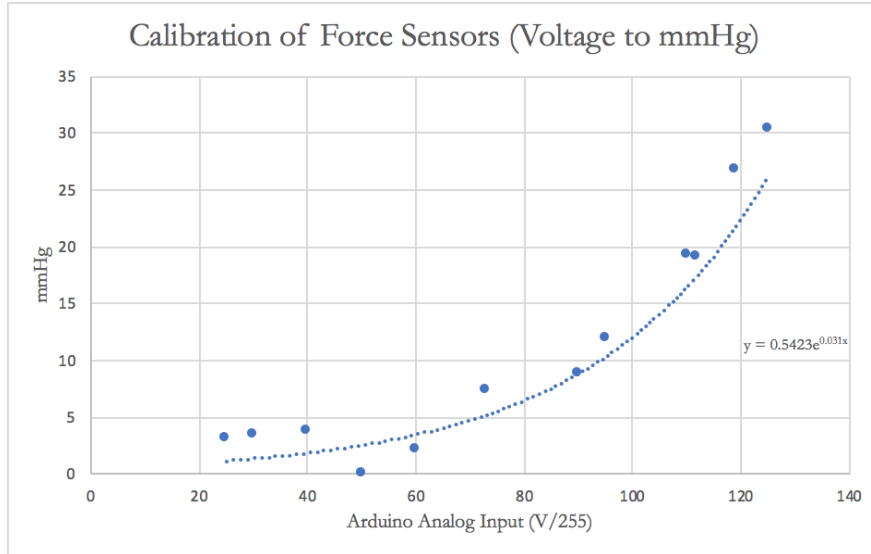


Figure 5.32: Force Sensor Calibration Curve w.r.t Pressure

Moisture Wicking tests

As explained above, a variety of sock models were considered, and aside from meeting critical design requirements for the effectiveness of measurements, other characteristics of the sock were taken into account to make a choice regarding the optimal sock. As explained in the Objectives section, the team desired to produce a product that displayed a high level of comfort for the user. The first metric for comfort in a sock that the team assessed was the sock's ability to wick away any moisture. While there are certain sock designs available for moisture-management in socks such as US Patent #5353524A, the team felt that comparing socks currently available on the market would lead to results satisfying the originally laid out requirements. As such, the team selected the top performing socks from the Sock Pressure Tests, and performed standard Moisture Wicking Tests on them. The socks were mildly dampened at room temperature and pressure with water heated to ~ 37 C (normal body temperature). The weight of the socks was logged over time until the socks dried up. The ideal sock would exhibit a higher rate of change in weight (i.e. least water retention capacity). As a linear relation appeared, it became clear that in the interest of beginning the test with the socks all containing moisture to the same extent, the socks were completely soaked both manually and were left to sit submerged in the water basin for 60 min. For the sake of comparison, the normalized weights of the socks were compared over time. The results shown in Figure 5.33 show that the chosen EUROS sock performed the best under the conditions provided.

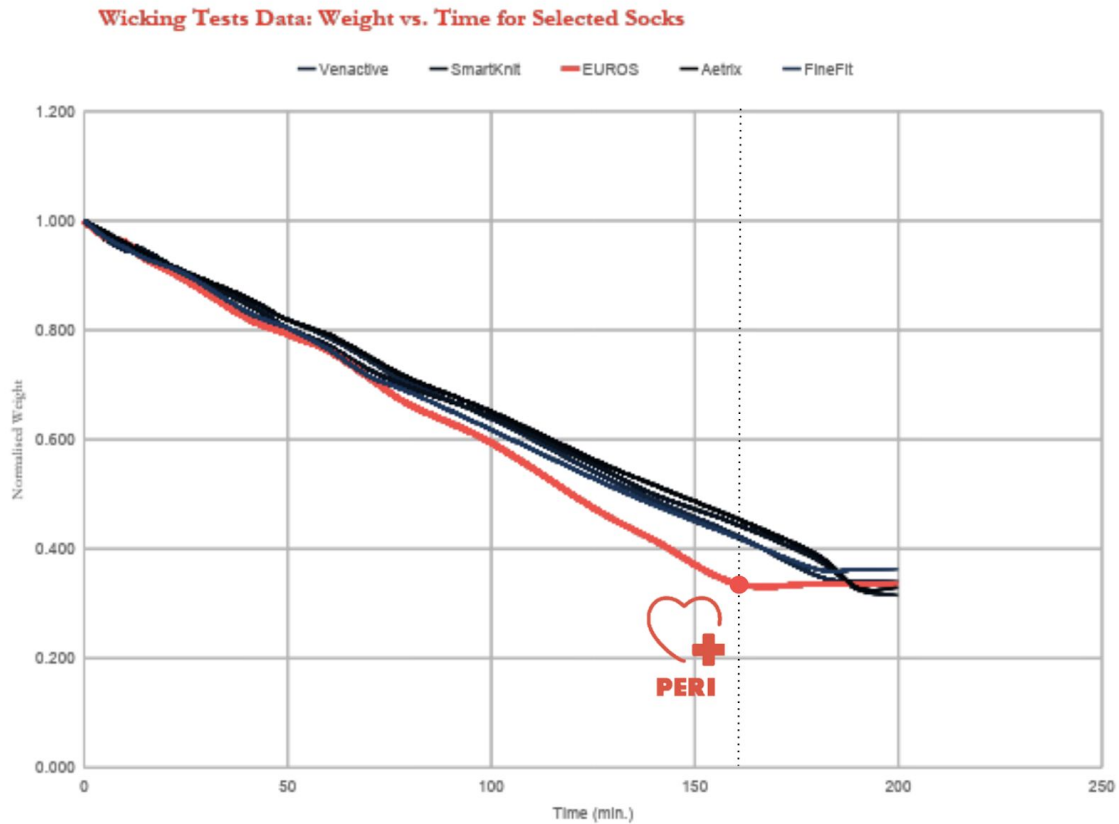


Figure 5.33: Wicking Test Data: Weight vs. Time for Selected Socks

Heat Dissipation Tests

In addition to the moisture wicking test, another central component to designing a comfortable product for the patient was finding a design whose heat dissipation characteristics met the initial requirements set forth - the sock is intended to be worn by the patient for an extended period of time. Therefore, heat dissipation tests were conducted on the set of socks touched on above. This test helped determine the thermal conductivity of the selected socks. The socks were fitted onto a 1L plastic bottle filled with water heated to ~70 C (to ensure plastic doesn't deform), and the temperature change over time was logged over time until the water reached room temperature, ~25 C. This setup is shown in Figure 5.34.



Figure 5.34: Heat Dissipation Test setup

The method of conductive resistance was used to determine the thermal conductivity of the socks. The ideal sock would have the highest thermal conductivity, that is the sock that retains heat the least. As can be seen in Figure 5.34, the socks performed very similarly with one exception, the Aetrex model. Fortunately, the Aetrex model was also one of the poorest performers in the Moisture wicking test as well and was no longer up for contention. Given that the EUROS sock was well ahead of the others in terms of the other tests conducted, this test served to make sure that the desired outcome would be achieved. Indeed, the EUROS sock was the second best performer by a tight margin. This finding left the team confident with the decision to stay with the EUROS model.

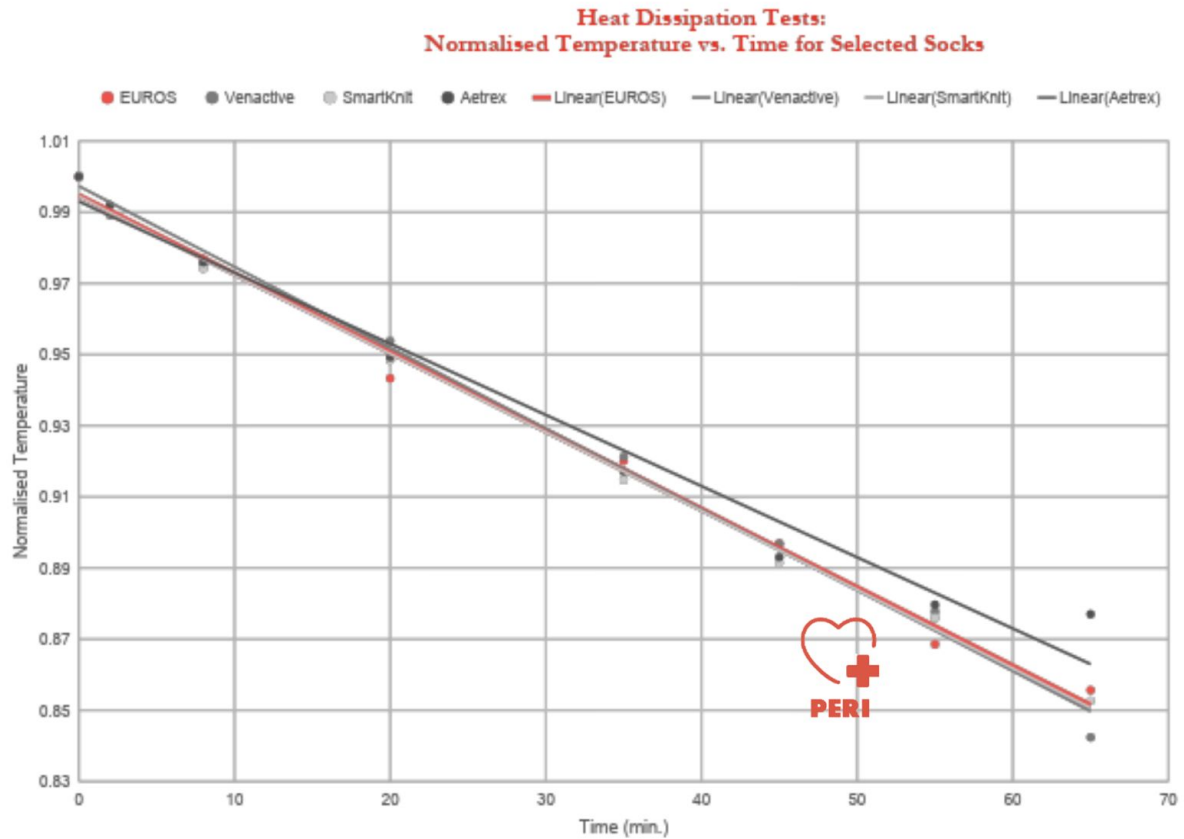


Figure 5.35: Sock Heat Dissipation Test

Electronics Module

Communication System

As mentioned before, the electronics module was an essential part of the project, being the basis for data acquisition and the biggest obstacle towards creating a comfortable device. The ideation towards the team's final, optimized, electronics module was an arduous multi-stepped process.

The first main design feature that had to be decided upon was the communication system from the three main systems: Cellular Data (4G), WiFi, and Bluetooth. The team quickly found that using Cellular Data would only be feasible if the device were to have a large, rechargeable battery, as the power consumption is much higher than the other two methods. Therefore, further research was only done into WiFi and Bluetooth, more specifically, WiFi Xbee and Bluetooth Low Energy, the two low-power versions of the respective systems. The research yielded the results summarized in the below table:

Table 5.5 - BLE vs WiFi Xbee

Specifications	Bluetooth Low Energy	WiFi Xbee
Requires Parts Besides SmartPhone/Module	No	Yes (WiFi Network)
Emission Distance	~10 m	~100+ ft
Data Speed	20-30 times slower than WiFi	Real-Time
Power Consumption (10 Packets a Day)	50 mW	500 mW

Note: table values found from Samosuyev[55] and B. Ray[56]

A WiFi device requires that the patient have access to a WiFi network at all times, which is not always the case. If not, the device would have to back-store data, which would cause an increase in power consumption. It is more likely that a patient carry a bluetooth module, or cell phone around with them at all times. While WiFi has a faster data transfer rate than bluetooth, this meant very little to the team, as data being delayed by a factor of milliseconds is irrelevant. However, the 100+ meters of emission data with WiFi would enable the user more travel space without needing to carry a cell phone. Therefore, further power calculations were done to see if WiFi with back logging would be feasible.

The power calculations were completed based on a circuit found on the Electronic Design[57], which was used for a similar application, sending temperature data over a BLE device. The circuit is shown in Figure 5.36 below:

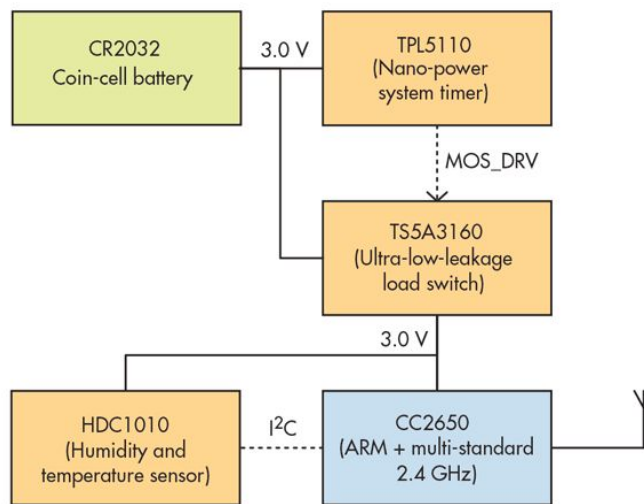


Figure 5.36 - Circuit from Electronics Design

The circuit essentially uses an ultra-low power leakage switch (TPL5110), which is activated by a nanotimer (TS5A3160) every so often. This activation allows the system to transfer data from a humidity and temperature sensor (HDC1010) via serial connection to a bluetooth low energy device (CC2650). The typical power consumption of a BLE device and ZigBee device were taken from a paper published by Microsoft, where the authors simply sent data periodically from a sensor node and found the current draw (Dementyev, 4). The power consumption of each device is shown below:

Table 5.6 - Power Consumption Comparison

Device	Active Current	“OFF” Current
TPL5110	~35 nA	N/A
TS5A3160	N/A	~2 nA
BLE	4.5 mA	0.00078 mA
ZigBee	9.3 mA	0.00180 mA

Assuming the device were to collect a reading every 5 minutes for 5 seconds, which is a very conservative estimate, the following two calculations could be made for each circuit.

$$I_{total} = I_{switch} + I_{timer} + I_{comm}$$

Where,

$$I_{switch} = 2 \text{ nA}, I_{timer} = 35 \text{ nA}$$

$$I_{ble} = (4.5 \text{ mA} * 60 \text{ seconds} / 3600 \text{ seconds}) + (0.00078 \text{ mA} * 3540 \text{ seconds} / 3600 \text{ seconds}) = 0.076 \text{ mA}$$

$$I_{zb} = (9.3 \text{ mA} * 60 \text{ seconds} / 3600 \text{ seconds}) + (0.00180 \text{ mA} * 3540 \text{ seconds} / 3600 \text{ seconds}) = 0.157 \text{ mA}$$

The zigbee consumes about twice as much power as BLE communications. This made a huge difference to us, as we wanted a device that did not require a rechargeable battery. Also, these calculations were made for a barebones ideal system, and factors that could come into play with a WiFi network, like backlogging, could increase the power consumption exponentially. This, along with the requirement of a network for WiFi devices, resulted in the team selecting BLE.

App Integration

An app was also created to display the analog data sent by the electronics module. This was done using the Arduino IDE and pFoddApp v3 and pFoddDesigner. The apps allow for both active connectivity with the BLE Nano V2, and the generation of a custom display using the “Create Menu” feature shown below in Figure 5.37.

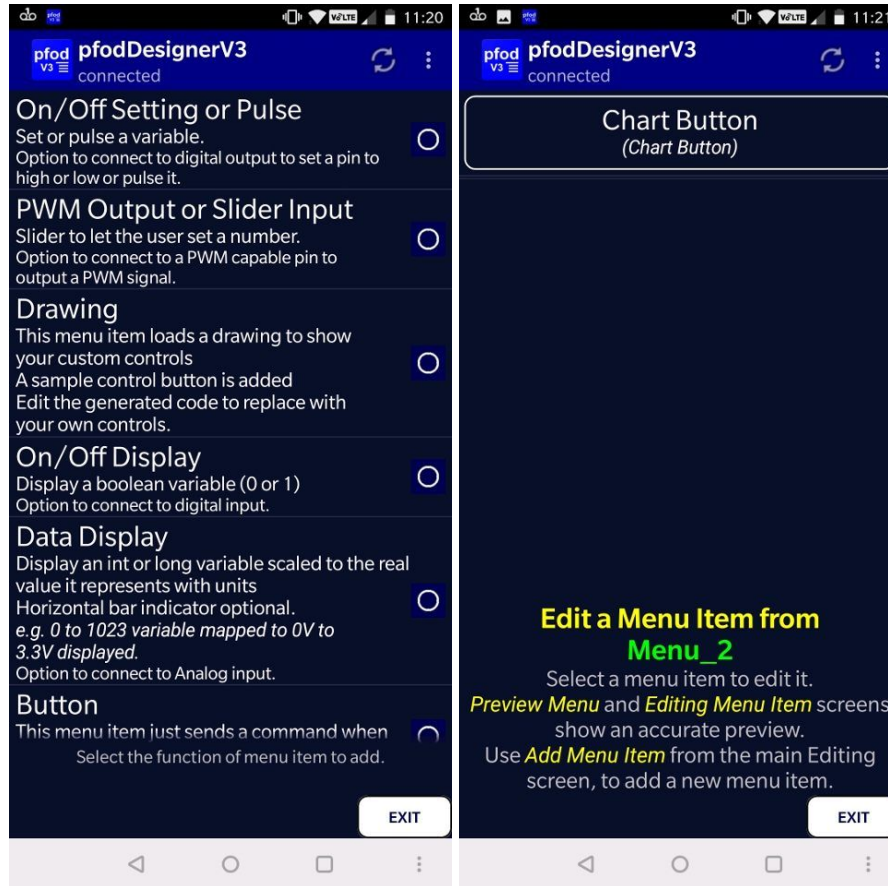


Figure 5.37 - Image of pFodApp V3

The app then allows the user to select pins for analog readings and create graphs, and creates Arduino code that can be exported to the IDE. The team downloaded the code, and made the following changes:

- 1) Added an analog pin for stretch sensor readings
- 2) Added a digital pin for specifying the end of data acquisition to the nanotimer (will be discussed with circuit)
- 3) Removed delay for data readings automatically set
- 4) Changed axis titles and set analog values to range from 0-256, rather than 0-1024, which is not compatible with the BLE Nano V2

The final app that was generated can be seen below as well., in Figure 5.38. The app was purely used for validation, to make sure that the device could properly export accelerometer and stretch sensor data. The top two graphs display the accelerometer data and the bottom displays displacement data. The code can be found in Appendix D.

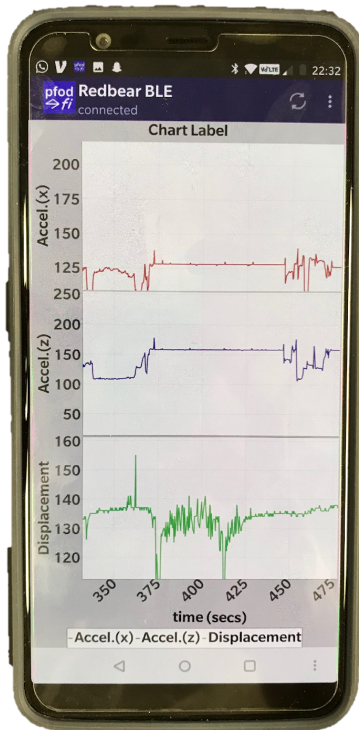


Figure 5.38 - Image of App Display

PCB/Circuit

For the first iteration of the electronics module, a similar circuit to the PCB was used. However, the accelerometer and nanotimer were on breakout boards, making it easy to prototype with them. The switch was completely absent. For the PCB, the breakout boards were stripped down to their chips, and the switch was included to further reduce power consumption. However, the team decided to keep the BLE Nano v2 nRF52832 bluetooth chip separate from the PCB, as the BLE chip on the Nano v2 took up most of the breakout surface area, and thus, very little space would have been saved. Also, this setup allowed the team to program the chip easily. The total circuit is shown in Appendix B. The inputs and outputs of the PCB are as following:

Inputs - 3 Volts, Ground

Outputs - DELAY, DONE, COM, SDA, SDO, SCL, CS

These pins and the entire circuit will be explained in depth, starting with the TPL5110 mentioned earlier:

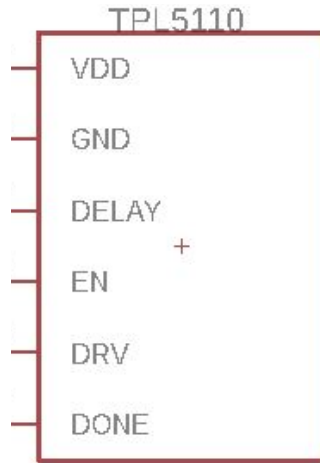


Figure 5.39: TPL5110 - Ultra-Low Power Nanotimer

VDD

The VDD pin powers the nanotimer directly from the battery

GND

The GND pin is always grounded.

DELAY

The DELAY pin is connected to an output of the PCB, giving the user the option of deciding what it is connected to. The pin itself is used to determine the frequency that the timer runs measurements. This is done by varying the resistance between the pin and ground, using the equation below. In this equation, T is the desired time, while R_{ext} is the resistance connected to ground. The chip sends current through the resistor when it is first powered to determine R , and thus, the sampling time. Coefficients a , b , and c , vary based on ranges of measurement times, shown in the table below the equation.

$$R_{EXT} = 100 \left(\frac{-b + \sqrt{b^2 - 4a(c - 100T)}}{2a} \right)$$

Table 5.7 - Coefficients for Delay Pin

SET	Time Interval Range (s)	a	b	c
1	1 < T ≤ 5	0.2253	-20.7654	570.5679
2	5 < T ≤ 10	-0.1284	46.9861	-2651.8889
3	10 < T ≤ 100	0.1972	-19.3450	692.1201
4	100 < T ≤ 1000	0.2617	-56.2407	5957.7934
5	T > 1000	0.3177	-136.2571	34522.4680

EN

Setting the EN pin to high allows the device to act as a timer.

DRV

The DRV pin is set high whenever the timer reaches the desired data acquisition time.

DONE

The DONE pin is connected to an output pin on the PCB, and from that, a pin on the BLE Nano V2. When the output pin is set high, the timer is notified that the module is done collecting data, and enters sleep mode until the timer triggers DRV again.

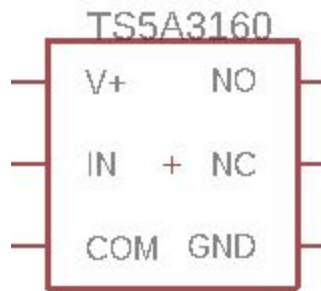


Figure 5.40: TS5A3160 - Ultra-Low Leakage Switch

V+

The V+ pin powers the switch directly from the battery.

IN

The IN pin is directly connected to the DRV pin on the nanotimer. When this pin is low, the switch connects COM and NC. When this pin is high, the switch connects COM and NO. Therefore, when the nanotimer activates and sets the DRV pin high, the switch connects COM and NO, and when readings are not being taken, the switch connects COM and NC.

COM

The COM pin is connected directly to the battery. As mentioned above, it is connected to NC when the IN pin is low, and connected to NO when the IN pin is high.

NO

The NO pin is connected to power the accelerometer chip, as well as to an output of the PCB, which allows the BLE Nano V2 to be powered. This means that the accelerometer and BLE Nano V2 only activate when the nanotimer triggers the switch to open, and turns back off when the switch is closed.

NC

The NC pin is not connected to anything, meaning no current flows when the switch is off.

GND

The GND pin is always grounded.

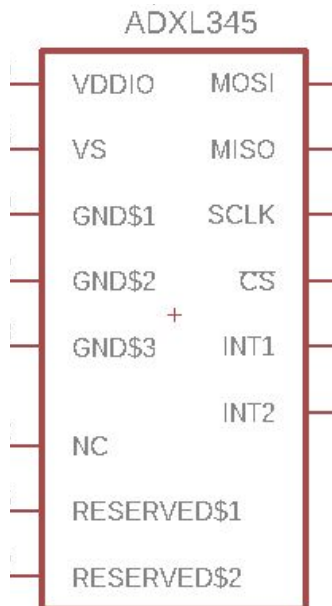


Figure 5.41: ADXL345 - Low Power Accelerometer

VDDIO

As mentioned before, the VDDIO pin is directly connected to the NO pin of the switch. This pin powers the digital functions of the accelerometer.

VS

This Vs pin is connect the same way as the VDDIO pin, and turns on the accelerometer every nanotimer cycle. While connecting the Vs pin and VDDIO pin to the same power source is not the best practice due to noise generation, for the purposes of this project, where the exact accelerometer values are not as important as the trend, the noise was ignored.

GND 1, 2, 3

The GND pins are always grounded.

NC, RESERVED 1, 2, INT 1, 2

Not Connected

MOSI/MISO/SCLK/CS

These four pins are used for SPI serial communication, and are outputs of the PCB, meant to be connected to the BLE Nano V2. In SPI communication, the CS pin is set low by the Master (BLE) when data transmission begins, and set high by the Master when completed. In three wire SPI, signals are sent between the two using the SDIO pin, while four wire SPI uses both the SDI and SDO pins. The SCLK pin controls the timing of the data acquisition, and thus the sampling rate. As our circuit only requires the ADXL345 to send signals to the BLE and not vice-versa, the three wire SPI was chosen. The MISO pin acts as the SDIO pin. The BLE Nano V2 has three pins specified for SPI that would be connected to MISO, SCLK, and CS.

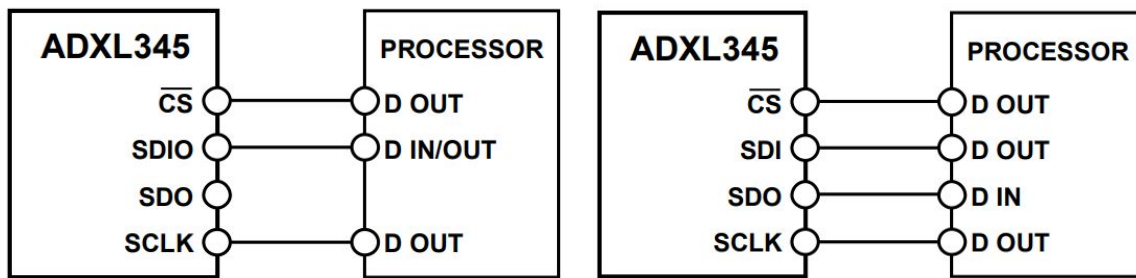


Figure 5.42: Left - 3 Wire SPI, Right - 4 WIRE SPI

The final board file is shown in Figure 43, alongside the actual board. Unfortunately, the team did not have time to implement the SPI interface with the board. However, the board was implemented to activate the BLE Nano V2 every 10 minutes, validating the other parts of the circuit. The power consumption tests to be discussed in validation showed that the board could be used to double the battery the life time. It also would reduce the overall volume of the electronics module by a factor of 6.

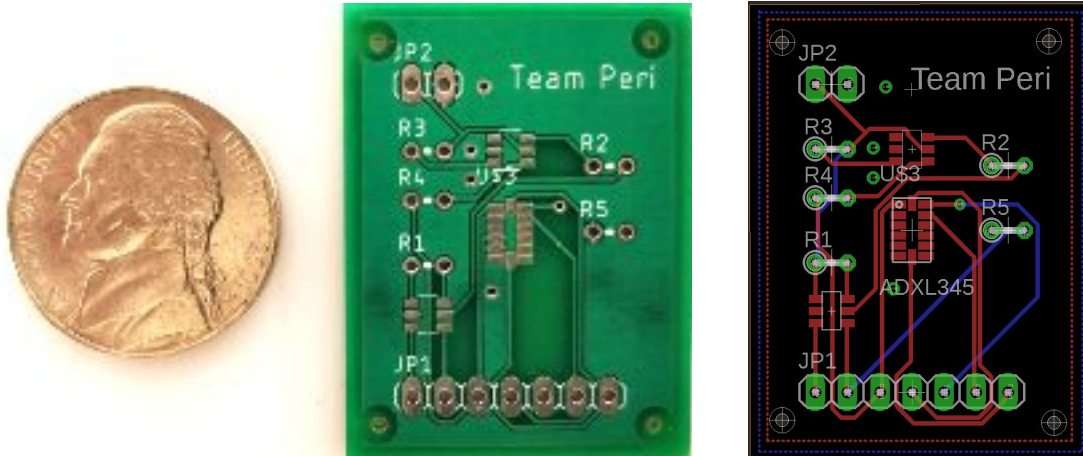


Figure 5.43: Electronic Module PCB

Sock Sewing

In order to put the sock and the electronics module together, the team sowed two main components together:

- **Resistance band:** in order to integrate the resistance band to the sock, the team carefully placed it 7 cm above the medial malleolus and sowed a piece of extremely elastic fabric (100% Lycra Spandex) on top of it to secure it while letting it stretch freely. In this way, the team was able to protect the resistance band from the environment while securing it at the right position on the sock. Moreover, in order to make sure that the measurements for the change in diameter were accurate and consistent, the team fixed both ends of the resistance band by firmly sewing them to the sock and sewing the attachments points together to prevent relative motion between the two ends.
- **Electronics Module Casing:** in order to secure the electronics module, the team manufactured a case made of silicon that would minimize the exposure of the electronics board to the environment and the sock. The electronics board was placed inside the silicon casing, which was in turn placed inside a fabric compartment with a velcro opening that was sewed to the side of the sock.

5.6.6 - Final Design



Figure 5.44: Sock Final Design

6. Validation and Testing

6.1 - Pressure Tests on Final Sock

To further validate the pressure profile of the final sock chosen, EUROS, the same pressure tests applied for down-selecting socks was performed using the final sock form comprised of sewn conductive fabric, magnetic connection terminals, stretch sensor, and attached electronics module, velcro cover, and pressure optimal fabric. In reiteration, the purpose of the pressure tests conducted on the sock's final form was to determine the range of pressure applied by the sock at maximum diameter using the large leg model as an upper bound and the small leg model as the lower bound. Figure 6.1 below shows 10 points along the leg model, one for each rod arm, where a force sensor was placed. As before, voltage measurements were calibrated into mmHg values using the calibration curve created using socks of known pressure and wrapping those on the leg model (Figure 5.32).

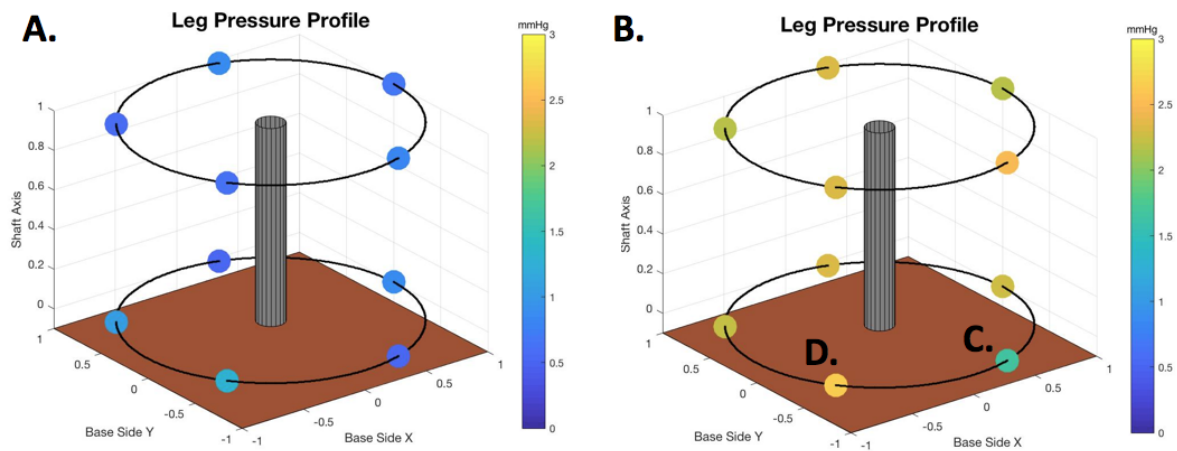


Figure 6.1: Final Sock Pressure Tests. (A) Leg Pressure Profile at smallest diameter allowed by the leg model developed. (B) Leg Pressure Profile at largest diameter allowed by the leg model developed. (C)(D) Artifacts of variability in measurement.

It can be concluded from these results that the range of pressures from the final Peri Smart Sock lies within the range of 0.94-2.38 mmHg, which at its maximum is 29.75% of the threshold set of 8 mmHg known to displace leg fluid over time and cause skin indentation.

Let it be observed, as well, that there is some discrepancy between each force sensor reading. Part of that stems from noise since the mean calibration curve was used for all force sensors as explained before. Moreover the socks were placed upside down onto the shaft such that the sensors closest to the X-Y plane would be closer to sock opening, so for reference, the X-Y plane resembles the area closest to the knee while the top one would be near the medial malleolus. This placement could have caused variability in measurement because a leg is not circular in nature nor is pressure evenly distributed throughout a sock due to weaving/sewing specifications in manufacturing. The green dot in Figure 6.1 labelled C. is an example of artifact that proves this point. Building on this idea, the electronics module attached to the final version of the sock could have led to the brighter dot lying left of the green one labelled D. This would seem appropriate because applying greater pressure on one part means that the fabric is undergoing higher shear stress at the edges of the rod arm faces. Consequently, the dots sensors closest to this effect will read smaller pressure measures as the profile skews itself to D.

6.2 - Foam Model Validation Tests

To validate the foam models, pitting tests were conducted on both the industry standard edema models and the corresponding foam models. The force vs. displacement data collected was then

analysed to assess how accurate the foam models simulated actual edema. The plots presented in the Figures 6.2 to 6.5 below show the results.

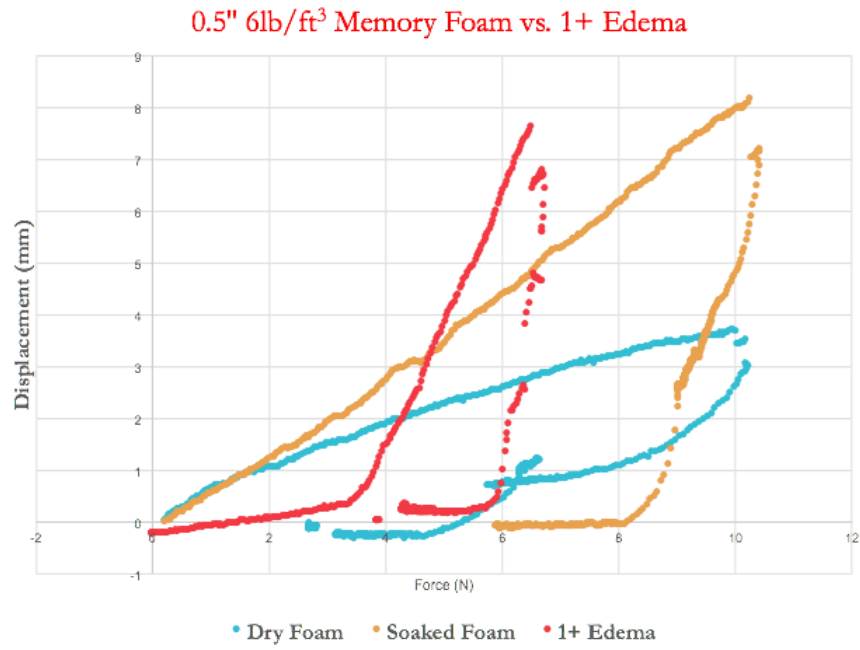


Figure 6.2: 0.5" 6lb/ft³ Memory Foam vs. 1+ Edema

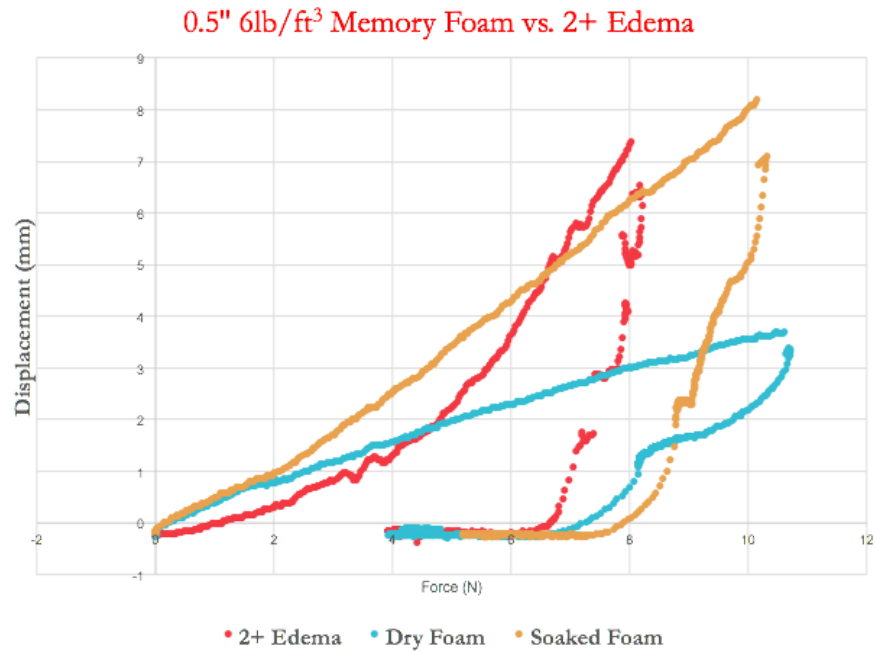


Figure 6.3: 0.75" 6lb/ft³ Memory Foam vs. 2+ Edema

0.5" 6lb/ft³ Memory Foam vs. 3+ Edema

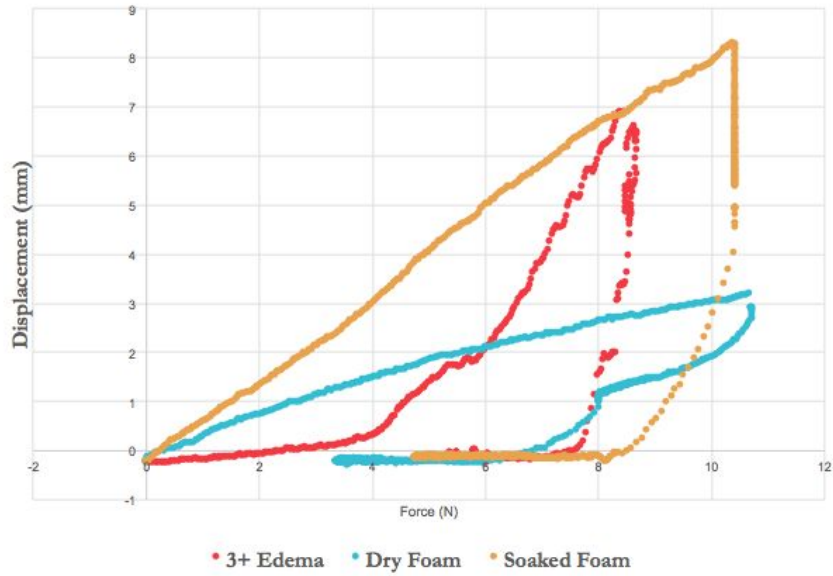


Figure 6.4: 1.00" 6lb/ft³ Memory Foam vs. 3+ Edema

0.5" 6lb/ft³ Memory Foam vs. 4+ Edema

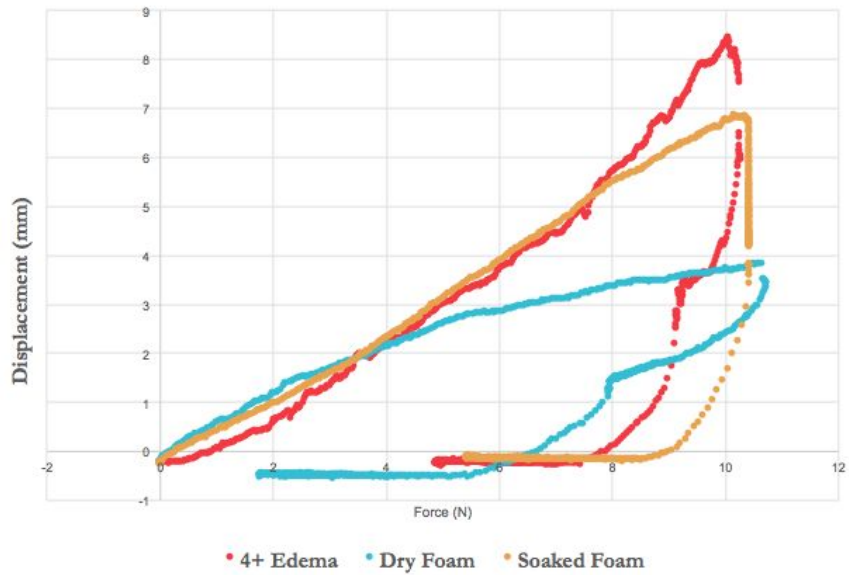


Figure 6.5: 1.25" 6lb/ft³ Memory Foam vs. 4+ Edema

Referring to the figures above, it can be observed that the 1.25” 6lb/ft³ memory foam model closely simulates 4+ edema. However, the other foam models are inaccurate.

6.3 - Sock Measurement Precision Tests

In order to validate the precision objectives stated in the objectives section of the report, the team first carried out a linear displacement test on the resistance stretch sensor. In order to do this, the stretch sensor was connected to an arduino analog input via a voltage divider circuit using a resistance of 10 KOhms. The sensor was then elongated to a resting position and placed alongside a ruler. Following this, the stretch sensor was manually displaced until the arduino read-out increased by a unit of 1 and the displacement of the sensor was recorded. This was then repeated at several different baseline lengths. The purpose of this test was to record the minimum linear displacement that is detectable by the sensor. The team was able to find a measurement precision of 3.0mm, a precision that fell well below our reach objective of 6.0mm measurement precision.

Given the results of the linear displacement tests described above, the team was expecting a minimum radial displacement of about 0.50mm to be detected. This expected radial displacement was tested using the leg model. The stretch sensor was placed around the model while in its unexpanded position. The leg model was then gradually expanded using the rack and pinion mechanism until the arduino digital output increased by a unit of one. This precision test resulted in a minimal detected radius displacement of 1.00mm. This result was half a millimeter above our expected precision calculated from our linear displacement test, and can most likely be attributed to the low measurement precision of the leg model itself.

6.4. Power Consumption Tests

A power consumption test was performed on both the initial circuit and the PCB (see Table 6.1). The first test was performed by placing a multimeter in series with the battery and the power pin of the nano-timer on the initial circuit. The second was performed by placing the multimeter in series with the battery and the power input of the PCB. Something to note is that while the PCB was not fully integrated, the accelerometer was still sending out serial packets. Because the system does not require two-way data acquisition, this is believed to be an accurate representation of the power consumption of the PCB.

Table 6.1: Power Consumption of Boards

Board	Power Consumption
Initial Board	15.4 mA
PCB	7.6 mA

After talking to Dr. Cacchione, the team decided on a data acquisition frequency of every 10 minutes. While it would be simple to take just one measurement to maximize battery life, the team decided that measurements for 5 seconds would allow accurate accelerometer data filtration, . Therefore the calculations below were completed. One thing to be noted is that for both boards, the current draw while the nanotimer was not active was $< 1 \mu A$, as expected, and could not be detected by the multimeter. Because of the very small effect of this value, it was ignored.

$$I_{board} = (15.4 \text{ mA} * 50 \text{ seconds} / 3600 \text{ seconds}) = 0.2139 \text{ mA}$$

$$I_{PCB} = (7.6 \text{ mA} * 50 \text{ seconds} / 3600 \text{ seconds}) = 0.1055 \text{ mA}$$

These calculations were then used to find the battery life of each board using common battery power values found on DigiKey and Mouser. Because of the size limitation of the project, the team decided to use coin cell batteries. The values are found below:

Table 6.2: Power Consumption of Boards

Standard Battery mAh	Board Battery Life	PCB Battery Life
40	7	15
55	10	21
100	19	39
210	40	82
265	51	104
560	109	221
620	120	244
1000	194	394

Within size constraints, a large battery was concluded to be better than a small one. The size of the largest battery (radius of 24.5 mm) was well within the constraints of the electronics module. The weight was also very small, and therefore, the 1000 mAh battery was chosen.

7. Discussion

7.1. Target vs Accomplished Performance

7.1.1. Sock

1) Greater precision measurements from sock

As stated in the Objectives section, the goal that the team set for itself was to obtain a measurement precision of 6.3 mm for the leg perimeter. As explained in section 5.6.4.3, the final system form contained a sensor capable of detecting a change in perimeter of 2 mm.

2) Resistance band vs. capacitance band (Lower cost)

This was also achieved with a sensor ranking below in the initial cost estimates set forth in the Binding Project Proposal. Indeed, the team found that it was able to successfully integrate a resistance band in the sock's final form without the need to use a capacitance band. In addition, the team was able to address its concern that it would have difficulty converting the output from a resistance band, which scales quadratically with length, compared to converting the output from a capacitance band, which scales linearly with length. Finally, being able to use a resistance band rather than a capacitance yields significant advantages in terms of cost. The resistance bands used in the team's experiments ranged from \$3 to \$20 (the resistance band selected for the final product cost \$12), whereas the capacitance bands that the team was considering ranged from \$100 to over \$300.

3) Communication and connectivity achieved

The team was also able to connect the final system to an external device wirelessly, rather than having the connectivity to the controller be wired, which was initially stated as a reach goal. The team achieved this by using a Bluetooth LE on the sock to connect to a mobile device - an Android phone in this case. Another endeavor that made this possible was using a fully integrated PCB that allows all of the required equipment to be worn on the sock, rather than having an external Arduino connection to the sock, which had been considered a possibility for proof of concept in the restrictions on this project.

4) User Comfort, best in its class of socks,

The team had initially set out to design a sock that was considered highly comfortable by its users, aiming for their high satisfaction. While the team seems to have met its goal, it first had to define new metrics by which to measure this. The three metrics that the team considered were the pressure that the sock applies to the leg, where a lower pressure represents a greater level of comfort, the ability of the sock to wick moisture, where a sock able to wick moisture at a faster rate would be more comfortable, and finally heat retention, where a sock that dissipates heat at a greater rate is more comfortable. These comparisons were made across several sock models chosen for their

comfort in customers requiring high levels of comfort due to conditions such as diabetes for example. The tests showed that the chosen socks ranked as applying the least pressure to the leg, the best at wicking moisture and the second-best at dissipating heat, which satisfied the initially stated requirements.

5) Pressure Constraints achieved

As stated above, the pressure that the sock applied was taken into consideration when on the account of comfort. However, the pressure applied by the final sock was also of great importance to the precision of the device measurements, as explained in the section above. Indeed the sock chosen for the final model applied a pressure well under the maximum 8 mmHg allowable.

6) Detachable Module vs Integrated

Finally, the final design of the sock included the integration of the electronics module on the sock itself rather than on an external platform, thus allowing to the device to fully remotely monitor, as the project was initially intending. Furthermore, the team was able to devise a design that allowed for the electronics module to be fully detachable. The following ensued in the washability of the system. Indeed, this removed the need for the electronics module itself to be waterproof and washable. The user would simply be able to remove the module from the sock before washing it. The team thus achieved its reach goal of having a fully washable device.

7.1.2. Custom MTS Machine

Table 7.1: Target vs. Accomplished Objectives for Custom MTS Machine

Description	Quantitative Objectives	Was Objective Realised?
Range of Normal Operating Force	0 N to 10 N	Yes, via the controlled use of a 12.7 mm stroke, 5lbf (22N) linear actuator
Resolution of Force Measurements	~0.01 N	Yes, via the use of a 0 → 10lbf (44.5N) range compression load cell
Displacement Range	0mm to 10mm	Yes, via the use of a 12.7mm stroke, 5lbf (22N) linear actuator
Resolution of Displacement Measurements	~2mm	Yes, via the use of a high resolution, 0 → 10.6mm travel, linear motion potentiometer
Indentation Speed Control	Controllable Speed with the range of 0 mm/s to 3 mm/s	Yes, via the use of a DC speed controller

Additionally, the MTS machine was cased for safety of use, and to also prevent damage to the circuitry.

7.1.3. Leg Model

Table 7.2: Target vs. Accomplished Goals for Leg Model

Description	Quantitative Objectives?	Was Objective Realised?
Radial Expansion Range	3.5 cm to 7.3 cm	Yes, via a radially expandable gear mechanism
Minimum Pressure Measurable	~8 mmHg	Yes, via the use of high resolution pressure plates
Edematous Lamination on Leg Exterior	Laminate Leg Prototype Exterior with artificial 0 to 4+ Edema	Yes, via the use of purchased edema pads

7.2. Recommendations

Expediting Patient Testing

One of the team’s key learnings during this process was the importance of identifying the key components of the project early, all while setting at least one realistically achievable backup plan. In the case of this project, the team had hoped to be granted an IRB approval in order to conduct in vivo testing on actual chronic heart failure. One of the most interesting aspects of the project, and one of the biggest challenges, was that there was often little to no previous research on the properties of edematous tissue. Therefore, being able to conduct testing on live patients would have been the ultimate source of validation for the team’s efforts. However, the IRB approval kept being delayed beyond expected, and was ultimately never approved in time for the project. The team was therefore left needing to find a new source for the missing piece in the project, which proved a very time-consuming endeavor late in the project.

As such, the team would highly recommend that any successor to this project follow this team’s efforts to obtain an IRB, all while bearing in mind the difficulties that it might impose on the team’s timeline. As mentioned above, being able to test on patients would ultimately allow to fully validate

the device, as there is currently little knowledge concerning the properties of edematous tissue. The potential successor to this project would not be required to alter the design of the current equipment to continue testing under an IRB as all components of the project were designed with the intention of moving forward with IRB testing. Furthermore, the IRB was submitted for the current equipment. The team would therefore recommend beginning any future endeavors with in vivo testing before going through any serious design changes.

Careful Outsourcing and Options

In addition to relying on an external entity to deliver the team's preferred method of validation, the team had also intended to work with Drexel's Shima Seiki Haute Technology Laboratory both to learn about textile manufacturing to help shape our final design, and to fully manufacture the sock. However, as explained in section 5.6.5.1, due to unforeseen complications in the relationship between Penn and Drexel, the team was unable to utilize this resource. Unfortunately, based on the positive tone of the discussions that the team had had with the laboratory, the team had been confident that the sock would be manufactured in the timeframe imposed by the project, and therefore did not continue exploring other options for manufacturing. This proved to be a costly mistake, as it left the team scrambling to find a local replacement that would be able to manufacture the sock in a short amount of time.

Both of the examples above show cases when the team concentrated all of its resources in one place and paid the price for it. Especially if working in a tight timeframe, the team would recommend exploring a wider variety of outsourcing options. However, having worked on manufacturing the sock itself, the team would recommend exploring external options to embed the sensor, wire and magnets in the sock. Manufacturing the sock itself, however, no longer appeared necessary after the team compared current socks of different pressures available on the market, as there were several options that met the team's requirements described in section section 4. Work was already put into developing those low-pressure socks by their manufacturers, making them fit for the needs of this project for the foreseeable future.

User Comfort Tests with Final Form

From the very beginning of the project, the team knew that it was crucial to develop a product that was sound not only in its engineering, but a product that would also stand a chance of success on the market, and for that the team knew that the sock would have to be comfortable. However, as the team was setting its comfort goals, it became clear that something as subjective as comfort would be very difficult to quantify. As explained in section 5.6.5, the team developed several criteria by which to evaluate the comfort of the sock. However, the team would highly recommend that any future endeavors in this project include spending time on developing more methods to evaluate comfort, as the team feels that the sock's comfort will ultimately be one of the deciding factors contributing to

the product's success. While there may certainly be more tests to evaluate comfort than applied pressure, moisture wicking or heat dissipation, the team would recommend considering supplying current chronic heart failure patients with the final form of the product to gauge their view on comfort. Short-term comfort, that is the patient's opinion on the sock's comfort after wearing it for less than an hour, would be able to be tested with the current IRB once it is approved. However, the team would also recommend that the any successors to the project consider conducting longer term comfort test with patients, that is over the course of several days, and possibly weeks, to compare the patient's feedback for different models of socks that met the critical pressure requirements described in section 4.

Long Term Creep Tests

Due to the timeline of the project, the team was unable to conduct tests to see how the sock changes with time. While the team selected its resistance band bearing in mind that it would be under slight strain for extended periods of time, the team was never able to explore the long term effects of strain on the product. While the product will not be subjected to high levels of strain or temperature throughout its use, the risk of substantial creep is mitigated. However, the team would highly recommend conductin creep tests on the product. For initial testing, the successors might use a creep-testing machine, but the eventually the team would suggest submitting a new IRB in order to be able to test creep in the product's actual environment, that is when it is subjected to the wear and tear of being worn by the patient for an extended period of time. This sort of test would be crucial in validating that the device does not stretch over time, which could lead to the device reading false negatives, that is not detecting an increase in leg diameter when it occurs, which would defeat the purpose of the device.

Improve Patient Feedback/Data Collection

The last two subsections describe recommendations that would have potential successors conduct long-term tests on patients in addition to the instantaneous form of testing that the team had already intended on carrying out. As mentioned before, this would require getting a new IRB approved, However, the team would highly recommend that this IRB include a wider variety of care centers or hospitals than the Mercy LIFE center. Indeed, while the center does provide a good source for testing, the patient body is relatively homogenous, due to the location of the center. It would also be useful to conduct testing on a wider variety of patients in order to get feedback that would more accurately represent the population at large. Indeed, receiving feedback from patients with higher resources could also contribute significantly to the design process, as they may offer a faster path to market in the short term.

8. Budget, Donations, and Resources

Bill of Materials	Price	Quantity	Total
Sock Prototype 1			
Arduino 101	39.95	1	39.95
Conductive Rubber Cord Stretch Sensor	9.95	1	9.95
Sock Prototype 1 Total			\$49.90
Sock Prototype 2			
BLE NANO V2 with Programmer	45.98	1	45.98
SparkFun ADXL345 Breakout	17.95	2	35.90
BLE NANO V2	16.95	1	16.95
ADXL335 Breakout	14.99	1	14.99
Adafruit Stretch Sensor	9.95	1	9.95
TPL 5110 Watchdog Breakout	4.95	2	9.90
TPL 5110 Watchdog Breakout	4.95	2	9.90
Stainless Thin Conductive Yarn	4.50	1	4.50
3V CR1220 With Leads	4.45	1	4.45
Sock Prototype 2 Total			\$152.52
Sock Prototype 3			
ADXL345 Chip	9.95	4	39.80
14" Flexible Stretch Sensor	20.95	1	20.95
12" Flexible Stretch Sensor	18.95	1	18.95
10" Flexible Stretch Sensor	16.95	1	16.95
Circular Knit Sensor Kit	15.00	1	15.00
CR2450	1.09	10	10.90
36" x 2" Purpose Elastic	5.96	1	5.96
IC Switch SPDT	0.99	4	3.96
IC Switch SPDT	0.99	4	3.96
TPL 5110 Chip	0.93	4	3.72
TPL 5110 Chip	0.93	4	3.72
Custom PCB	35.54	4	142.16
Sock Prototype 3 Total			\$286.03
Pitting Device			
Clamp Set Wall Mounts	73.99	1	73.99
Linear Actuator	69.99	1	69.99
Force Sensor	58.67	1	58.67
Bourns Slide Potentiometer	58.67	1	58.67
Cast Iron U-Shaped Supprot	39.00	1	39.00
DC Speed Controller	31.99	1	31.99
13 mm diameter aluminum rod	22.70	1	22.70
Surface Mount Hinge with Holes	4.83	4	19.32
Zinc-Plated Steel Corner Bracket	0.63	12	7.56
1 in Galvanized Corner Bracket	3.28	2	6.56
Velcro Strap	5.30	1	5.30
Pitting Device Total			\$393.75

Leg Prototype	Price	Quantity	Total
Force Sensor	51.45	5	257.25
Black Oxide 1215 Lead Free Shaft Collar	4.55	6	27.30
Leg Prototype Total			\$284.55
Fabrics			
Resistance Stretchy Fabric	24.95	1	24.95
4-Way Metallic Spandex	14.00	1	14.00
4-Way Stretch Vynil	14.00	1	14.00
2-Way Stretch Vynil	10.00	1	10.00
Novelty Spandex	10.00	1	10.00
Miliskin Matte	9.00	1	9.00
2-Way Metallic Spandex	9.00	1	9.00
2-Way Stretch Solid Velvet	9.00	1	9.00
2 Way Stretch Solid Velvet	9.00	1	9.00
Cotton Lycra	7.00	1	7.00
Soft Potentiometer Kit	6.95	1	6.95
Rayon Lycra	6.00	1	6.00
Stretch Solid Mesh	6.00	1	6.00
Stretch Lining	5.00	1	5.00
Fabric Polyester Lycra	1.00	4	4.00
Fabrics Total			\$143.90
Socks			
Various SmartKnit Socks	15.96	4	63.84
Various SmartKnit Socks	15.95	3	47.85
Various Aetrex Socks	14.76	3	44.28
Various Euros Socks	14.95	4	59.80
Various VenActive Socks	14.39	2	28.78
Various VenActive Socks	11.99	2	23.98
Socks Total			\$268.53
Testing Materials			
Ultra Highest Density Memory Foam	48.80	1	48.80
5LB Memory Foam	24.99	1	24.99
3LB Memory Foam	17.99	1	17.99
Pet Plastic Square Beverage (32 oz)	1.29	1	1.29
Pet Plastic Square Beverage (16 oz)	0.90	1	0.90
Pet Plastic Square Beverage (8 oz)	0.75	1	0.75
Testing Materials Total			\$94.72
Other Sources			
Rothberg Catalyzer - Socks	N/A		N/A
Rothberg Catalyzer - Breadboards	N/A		N/A
Dr. Cacchione - Edema Testing Kit	N/A		N/A
Adlab - 3D Printing	N/A		N/A
Total Spent			\$1,673.90

9. Intellectual property

The team has not and will not pursue any Intellectual Property Rights.

References

- [1]"Heart Disease and Stroke Statistics—2015 Update", American Heart Association, 2015.
- [2]S. Dunlay, N. Shah, Q. Shi, B. Morlan, H. VanHouten, K. Hall Long and V. Roger, "Lifetime Costs of Medical Care After Heart Failure Diagnosis", *Circulation: Cardiovascular Quality and Outcomes*, vol. 4, no. 1, pp. 68-75, 2010.
- [3]B. Jancin, "Acute heart failure mortality climbs with severity of peripheral edema", Mdedge.com, 2017. [Online]. Available: <http://www.mdedge.com/ecardiologynews/article/108605/heart-failure/acute-heart-failure-mortality-climbs-severity>. [Accessed: 01- Nov- 2017].
- [4]S. LeGare, "A Device for Measuring the Severity of Peripheral Edema", Degree of Bachelor of Science, Worcester Polytechnic Institution, 2007.
- [5]World Health Organization, "Global Atlas on Cardiovascular Disease Prevention and Control", 2017.
- [6]"Heart failure: When your heart doesn't work efficiently", Mayo Clinic, 2017. [Online]. Available: <https://www.mayoclinic.org/diseases-conditions/heart-failure/basics/definition/con-2002980> 1. [Accessed: 01- Nov- 2017].
- [7]"Heart Disease and Stroke Statistics—2013 Update", American Heart Association, 2013.
- [8]T. O'Brien, "Congestive Heart Failure Symptoms, Stages, Signs, Treatment & Causes", eMedicineHealth, 2017. [Online]. Available: http://www.emedicinehealth.com/congestive_heart_failure/article_em.htm. [Accessed: 02- Nov- 2017].
- [9]M. Roizen, "Forecasting the Future of Cardiovascular Disease in the United States: A Policy Statement From the American Heart Association", *Yearbook of Anesthesiology and Pain Management*, vol. 2012, pp. 12-13, 2012.
- [10]"Readmissions Reduction Program (HRRP) - Centers for Medicare & Medicaid Services", Cms.gov, 2017. [Online]. Available: <https://www.cms.gov/Medicare/Medicare-Fee-for-Service-Payment/AcuteInpatientPPS/Readmissions-Reduction-Program.html>. [Accessed: 02- Nov- 2017].
- [11]"Results from a State Scorecard on Health System Performance", The Commonwealth Fund Commission, 2009.
- [12]J. Vinson, M. Rich, J. Sperry, A. Shah and T. McNamara, "Early Readmission of Elderly Patients With Congestive Heart Failure", *Journal of the American Geriatrics Society*, vol. 38, no. 12, pp. 1290-1295, 1990.
- [13]"Assessing Edema and Documentation", Nrsg101.com. [Online]. Available: <https://www.nrsg101.com/assessing-edema.html>. [Accessed: 02- Nov- 2017].

- [14]K. Brodovicz, K. McNaughton, N. Uemura, G. Meininger, C. Girman and S. Yale, "Reliability and Feasibility of Methods to Quantitatively Assess Peripheral Edema", *Clinical Medicine & Research*, vol. 7, no. 1-2, pp. 21-31, 2009.
- [15]M. Lueck, Final Report Edema Swelling Measurement Device. 2010.
- [16]K. Labs, M. Tschoepl, G. Gamba, M. Aschwanden and K. Jaeger, "The reliability of leg circumference assessment: a comparison of spring tape measurements and optoelectronic volumetry", *Vascular Medicine*, vol. 5, no. 2, pp. 69-74, 2000.
- [17]H. Mayrovitz, "Limb Volume Assessments Based on Circumference Measurements: Possibilities and Limitations", 2012.
- [18]D. Hayn, F. Fruhwald, A. Riedel, M. Falgenhauer and G. Schreier, "Leg Edema Quantification for Heart Failure Patients via 3D Imaging", *Sensors*, vol. 13, no. 8, pp. 10584-10598, 2013.
- [19]F. Yu, A. Bilberg, L. Xiao and K. Yderstraede, "Foot edema simulation and monitoring using dielectric electro-active polymer sensors", *Sensors and Actuators A: Physical*, vol. 225, pp. 33-40, 2015
- [20]G. Mosti, H. Partsch, Compression Stockings with a Negative Pressure Gradient Have a More Pronounced Effect on Venous Pumping Function than Graduated Elastic Compression Stockings, In *European Journal of Vascular and Endovascular Surgery*, Volume 42, Issue 2, 2011, Pages 261-266, ISSN 1078-5884, <https://doi.org/10.1016/j.ejvs.2011.04.023>.
- [21]W. Yu, S. Kilbreath, R. Fitzpatrick and S. Gandevia, "Thumb and finger forces produced by motor units in the long flexor of the human thumb", *The Journal of Physiology*, vol. 583, no. 3, pp. 1145-1154, 2007.
- [22]"Classify Your Medical Device", [Fda.gov](https://www.fda.gov/MedicalDevices/DeviceRegulationandGuidance/Overview/ClassifyYourDevice/default.htm), 2017. [Online]. Available: <https://www.fda.gov/MedicalDevices/DeviceRegulationandGuidance/Overview/ClassifyYourDevice/default.htm>. [Accessed: 02- Nov- 2017].
- [23]"Class I / II Exemptions", [Fda.gov](https://www.fda.gov/MedicalDevices/DeviceRegulationandGuidance/Overview/ClassifyYourDevice/ucm051549.htm), 2017. [Online]. Available: <https://www.fda.gov/MedicalDevices/DeviceRegulationandGuidance/Overview/ClassifyYourDevice/ucm051549.htm>. [Accessed: 02- Nov- 2017].
- [24]"CFR - Code of Federal Regulations Title 21", [Accessdata.fda.gov](https://www.accessdata.fda.gov/scripts/cdrh/cfdocs/cfcfr/CFRSearch.cfm?fr=890.1575), 2017. [Online]. Available: <https://www.accessdata.fda.gov/scripts/cdrh/cfdocs/cfcfr/CFRSearch.cfm?fr=890.1575>. [Accessed: 02- Nov- 2017].
- [25]"How Much Does a 510(k) Device Cost? About \$24 Million", [MDDI Online](https://www.mddionline.com/how-much-does-510k-device-cost-about-24-million), 2017. [Online]. Available: <https://www.mddionline.com/how-much-does-510k-device-cost-about-24-million>. [Accessed: 02- Nov- 2017].
- [26]"Summary of the HIPAA Privacy Rule", [HHS.gov](https://www.hhs.gov/hipaa/for-professionals/privacy/laws-regulations/index.html), 2017. [Online]. Available: <https://www.hhs.gov/hipaa/for-professionals/privacy/laws-regulations/index.html>. [Accessed: 02- Nov- 2017].

- [27]R. Bryant and D. Nix, Acute & chronic wounds. .
- [28]E. Rabe, M. Stücker and B. Oetillinger, "Water displacement leg volumetry in clinical studies - A discussion of error sources", BMC Medical Research Methodology, vol. 10, no. 1, 2010.
- [29]W. Yuan, N. Zhou, L. Shi and K. Zhang, "Structural Coloration of Colloidal Fiber by Photonic Band Gap and Resonant Mie Scattering", ACS Applied Materials & Interfaces, vol. 7, no. 25, pp. 14064-14071, 2015.
- [30]"Vertical and AP Forces During Walking", 2017. [Online]. Available: <http://educ.ubc.ca/faculty/sanderson/courses/HKIN363/LABS/biomech/knmethod/ktcmeth.htm>. [Accessed: 02- Nov- 2017].
- [31]P. Current, "Penn engineers design material that could help diagnose concussions | Penn Current", Penncurrent.upenn.edu, 2015. [Online]. Available: <https://penncurrent.upenn.edu/2015-09-03/latest-news/penn-engineers-design-material-could-help-diagnose-concussions>. [Accessed: 02- Nov- 2017].
- [32]"Subminiature Gauging DVRT® | LORD Sensing Systems", Microstrain.com, 2017. [Online]. Available: <http://www.microstrain.com/displacement/sg-dvrt>. [Accessed: 02- Nov- 2017].
- [33]"Mouser Electronics - Datasheet", Mouser.com, 2003. [Online]. Available: <http://www.mouser.com/ds/2/187/honeywell-sensing-fs01-fs03-force-sensors-product--740269.pdf>. [Accessed: 02- Nov- 2017].
- [34]"Shopping", Baileyhydraulics.com, 2017. [Online]. Available: http://www.baileyhydraulics.com/prodcat/Hydraulic-Cylinders/type/Telescopic-Cylinder?gclid=EAIaIQobChMIqKik_NSg1wIVVWQZCh3QzwLFEAEYASAAEgI-hPD_BwE. [Accessed: 02- Nov- 2017].
- [35]"Products - Bimba Manufacturing", Bimba.com, 2017. [Online]. Available: <http://www.bimba.com/Products-and-Cad/>. [Accessed: 02- Nov- 2017].
- [36]E. Campo, Selection of polymeric materials. Norwich, N.Y: William Andrew, 2008.
- [37]J. Vondrejč, "Constitutive models of linear viscoelasticity using Laplace transform", Graduate, Czech Technical University in Prague, 2009.
- [38]Xu, D., et al., Sensing frequency design for capacitance feedback of dielectric elastomers. Sensors and Actuators A: Physical, 2015. 232: p. 195-201.
- [39]Ramin Fallahzadeh, Yuchao Ma, Hassan Ghasemzadeh, "Context-Aware System Design for Remote Health Monitoring: An Application to Continuous Edema Assessment", Mobile Computing IEEE Transactions on, vol. 16, pp. 2159-2173, 2017, ISSN 1536-1233.

- [40] Titler, M., Jensen, G., Dochterman, J., Xie, X., Kanak, M., Reed, D., and Shever, L., 2008, "Cost of Hospital Care for Older Adults with Heart Failure: Medical, Pharmaceutical, and Nursing Costs", *Health Services Research*, 43(2), pp. 635-655.
- [41] Eisner, L., 2018, "Wearables for Medical and Wellness Uses: Standards and FDA Guidance Documents", In *Compliance Magazine* [Online]. Available: <https://incompliancemag.com/article/wearables-for-medical-and-wellness-uses-standards-and-fda-guidance-documents/>. [Accessed: 28- Apr- 2018].
- [42] Grass, G., Rensing, C., and Solioz, M., 2010, "Metallic Copper as an Antimicrobial Surface", *Applied and Environmental Microbiology*, 77(5), pp. 1541-1547.
- [43] North, B., 2015, "The growing role of human factors and usability engineering for medical devices", *Human Centered Strategies*, BSI Group.
- [44] S. LeGare, "A Device for Measuring the Severity of Peripheral Edema", Degree of Bachelor of Science, Worcester Polytechnic Institution, 2007
- [45] K. Brodovicz, K. McNaughton, N. Uemura, G. Meininger, C. Girman and S. Yale, "Reliability and Feasibility of Methods to Quantitatively Assess Peripheral Edema", 2009. [Online]. Available: <https://www.ncbi.nlm.nih.gov/pmc/articles/PMC2705274/>
- [46] Kaulesar Sukul D.M.K.S, "Direct and indirect methods for the quantification of leg volume: comparison between water displacement volumetry, the disk model method and the fr... - PubMed - NCBI", *Ncbi.nlm.nih.gov*, 1993. [Online]. Available: <https://www.ncbi.nlm.nih.gov/pubmed/8277752>
- [47] W. Yuan, N. Zhou, L. Shi and K. Zhang, "Structural Coloration of Colloidal Fiber by Photonic Band Gap and Resonant Mie Scattering", 2015. [Online]. Available: <https://pubs.acs.org/doi/abs/10.1021/acsami.5b03289>.
- [48] P. Cacchione, "Project Proposal Meeting with Dr. Pamela Cacchione", Claire M. Fagin Hall, 418 Curie Blvd., 2017
- [49] "Plantar Pressure Mapping Sensor System", *Sensorprod.com*. [Online]. Available: <http://www.sensorprod.com/foot-plate-pressure-sensor.php>.
- [50] "3048L-4-502 Bourns | Mouser", *Mouser Electronics*. [Online]. Available: <https://www.mouser.com/ProductDetail/Bourns/3048L-4-502/?qs=%2fha2pyFaduiYp9E5NsQt4TQ2sz0BzedGNcZY99sF%2fFm1CxmfbTv1Sg%3d%3d>.
- [51] "Compression Load Cell", *Te.com*. [Online]. Available: <http://www.te.com/commerce/DocumentDelivery/DDEController?Action=srchrtv&DocNm=FC22&DocType=DS&DocLang=English>.
- [52] "12v Micro Linear Actuators | Progressive Automations", *Progressiveautomations.com*. [Online]. Available: <https://www.progressiveautomations.com/micro-linear-actuator?gclid=Cj0KCQiAl8rQBRDr>

ARIsAEW_To_11bk4mHIpThH7LBMcWu9Kr9URBvmu-gbLBHqU56dIfbRaU7Qbt8aAkrd
EALw_wcB.

- [53] "A Device to Assess the Severity of Peripheral Edema", 2007. [Online]. Available: <https://web.wpi.edu/Pubs/E-project/Available/E-project-042507-151149/unrestricted/DeviceToAssessPeripheralEdema2007.pdf>.
- [54] "The Sensoria Textile Pressure Sensors Technology", Sensoriafitness.com | Magnetic Attachment. [Online]. Available: <http://www.sensoriafitness.com/technology/>.
- [55] V. Samosuyev, "Bluetooth Low Energy Compared to Zigbee and Bluetooth Classic", Bachelor's, Mikkeli University of Applied Sciences, 2010.
- [56] B. Ray, "A Bluetooth & ZigBee Comparison For IoT Applications", Link Labs, 2015.
- [57] P. Pickering, "Designing Ultra-Low-Power Sensor Nodes for IoT Applications", Electronic Design, 2018. [Online]. Available: <http://www.electronicdesign.com/power/designing-ultra-low-power-sensor-nodes-iot-applications>. [Accessed: 30- Apr- 2018].
- [58] Robert G. Smith, F., 2018, "An Overview of Compression Hosiery", Uspharmacist.com [Online]. Available: <https://www.uspharmacist.com/article/an-overview-of-compression-hosiery>. [Accessed: 30- Apr- 2018].
- [59] Wu, S., Crews, R., Najafi, B., Slone-Rivera, N., Minder, J., and Andersen, C., 2012, "Safety and Efficacy of Mild Compression (18–25 mm Hg) Therapy in Patients with Diabetes and Lower Extremity Edema", *Journal of Diabetes Science and Technology*, 6(3), pp. 641-647.
- [60] S. Olsen, *The role of human factors in home health care*. Washington, DC: National Academies Press, 2010. 20 [Online]. Available: <https://www.ncbi.nlm.nih.gov/books/NBK210047/> [Accessed: 30- Apr- 2018]
- [61] 2018, [Online]. Available: <http://www.contourmd.com/Juzo-Size-Chart>. [Accessed: 30- Apr- 2018].

Appendix

Appendix A - Comparison of Peripheral Edema Assessment Methods

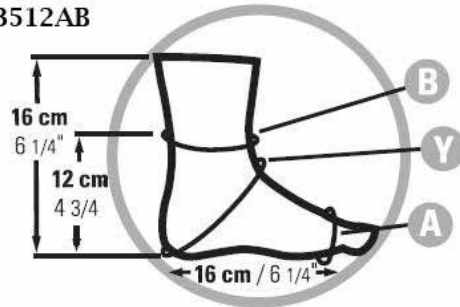
Below is a review of work that was conducted at the primary care clinic of Marshfield, Wisconsin, to evaluate methods of assessing peripheral edema for reliability, feasibility and correlation with the classic clinical assessment of pitting edema [14]. As explained in the body of the text, the eight methods reviewed in this comprehensive study were a classic pitting test, a patient questionnaire, measuring ankle circumference, the figure-of-eight method for measuring ankle circumference, a plain edema tester comprising a plastic card with holes of varying sizes pressed onto the skin, a modified edema tester using bumps rather than holes, indirect leg volume measurement calculated from measuring ankle and leg circumference, and measuring foot and ankle volume by water displacement. The conclusion of the study was that water displacement and ankle circumference were the most reliable method and had the lowest variability in diagnosis among clinicians. However, both methods display significant drawbacks due to the time and preparation needed for implementation.

Inter-examiner reliability was assessed with scatterplots of examiner 1 vs 2, Kappa statistics, and intraclass correlation coefficients (ICC) with 95% confidence intervals (CI) continuous measures. ICC was calculated based on three examiners assessing each patient and represents the expected reliability of a single examiner's rating (referred to as case 2.1 in Shrout and Fleiss 1979). Intra-examiner test-retest reliability was assessed by ICC as well. The tests were conducted on 20 patients with peripheral edema.

The result of the comparison showed that water displacement and ankle circumference had high inter-examiner agreement, which was shown by intraclass correlation coefficients of 0.93, 0.96 on the right and of 0.97, 0.97 on the left. The figure-of-eight method however lacked in agreement consistency, achieving only 0.64, 0.86. Indirect leg volume showed moderate consistency with 0.53, 0.66, and clinical assessments at all locations were generally low. Agreement was also low for the edema testers but varied by the pressure administered. Correlation with the classic, subjective clinical assessment was good for the nurse-performed assessments and patient questionnaire. Another important component of the study was that of the time required to make these measurements. It showed that ankle circumference and patient questionnaires each took 1 minute to complete. Other tools took over 5 minutes to complete.

Appendix B - Leg Sizing Chart

Juzo Malleo Ankle Support 3512AB



3512						
	1	2	3	4	5	6
	XS	S	M	L	XL	XXL
B	18-20 cm 7"-8"	20-22 cm 8"-8 3/4"	22-24 cm 8 3/4"-9 1/2"	24-26 cm 9 1/2"-10 1/4"	26-28 cm 10 1/4"-11"	28-30 cm 11"-12"
Y	27-29 cm 10 3/4"-11 1/2"	29-31 cm 11 1/2"-12 1/4"	31-33 cm 12 1/4"-13"	33-35 cm 13"-13 3/4"	35-37 cm 13 3/4"-14 1/2"	37-39 cm 14 1/2"-15 1/4"
A	18-20 cm 7"-8"	20-22 cm 8"-8 3/4"	22-24 cm 8 3/4"-9 1/2"	24-26 cm 9 1/2"-10 1/4"	26-28 cm 10 1/4"-11"	28-30 cm 11"-12"

Appendix C - PCB Diagram

